The Chilling Recount of an Unexpected Discovery: First Observations of the Plasma-Cascade Instability in the Coherent Electron Cooling Experiment

Irina Petrushina

Stony Brook University

August 1, 2019

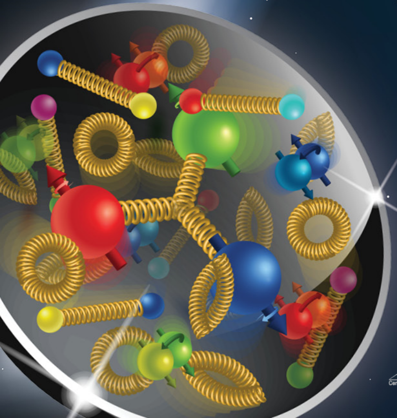

Electron Ion Collider – eRHIC

Contents

1. Project Overview
2. Accelerator Performance
3. Experiment with FEL-based System and Unexpected Result
4. Plasma-Cascade Instability
5. Future Plans and Conclusions

What is Coherent electron Cooling?

Short answer: stochastic cooling of hadron beams with bandwidth at optical wave frequencies: 1-1000 THz.

Long answer:

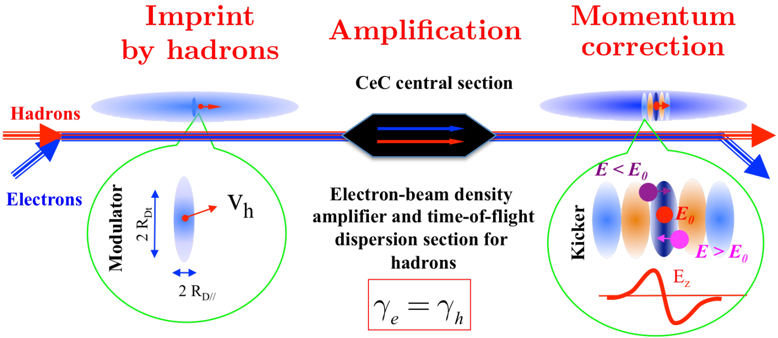

PRL **102,** 114801 (2009) PHYSICAL REVIEW LETTERS week ending 20 MARCH 2009

Coherent Electron Cooling

Vladimir N. Litvinenko[1,*] and Yaroslav S. Derbenev[2]
[1]*Brookhaven National Laboratory, Upton, Long Island, New York, USA*
[2]*Thomas Jefferson National Accelerator Facility, Newport News, Virginia, USA*
(Received 24 September 2008; published 16 March 2009)

CeC Proof of Principle Experiment

Goal: demonstrate longitudinal cooling of a single Au^{+79} bunch in the Relativistic Heavy Ion Collider.

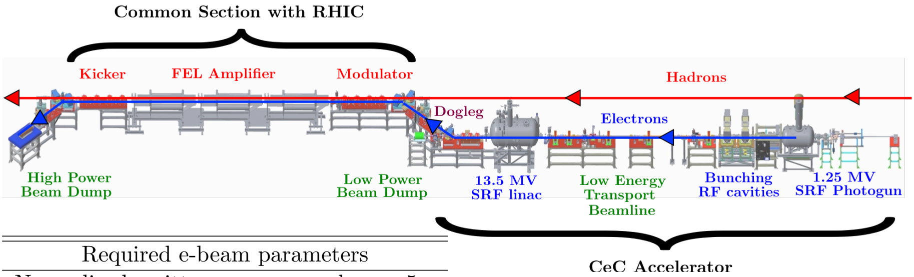

Required e-beam parameters	
Normalized emittance, mm-mrad	<5
Relative energy spread σ_E/E	10^{-3}
Bunch charge, nC	0.5-1.5
Pulse repetition rate, kHz	78
RMS bunch length, ps	10-50
Peak current, A	>75
Kinetic energy, MeV	14.5
FEL wavelength, μm	30

Hadron beam parameters	
Energy, GeV/u	27
Intensity, hadron/bunch	10^9
RMS bunch length, ns	5
Revolution frequency, kHz	78

CeC Accelerator

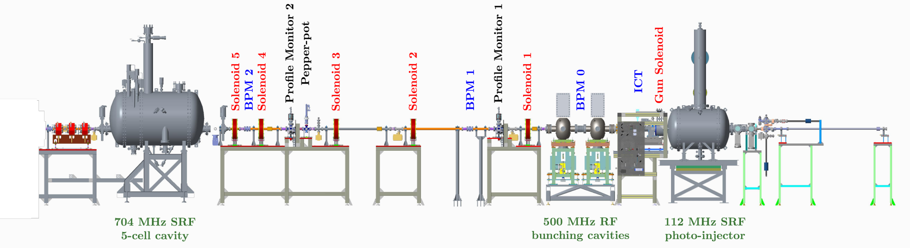

- 113 MHz SRF gun with CsK_2Sb photocathode. Cathode operation—weeks.
- 532 nm drive laser.
- Two 500 MHz copper cavities for ballistic compression to the required peak current.
- 704 MHz SRF accelerator cavity.

Demonstrated e-beam parameters	
Normalized emittance, mm-mrad	3-4
Relative energy spread σ_E/E	3×10^{-4}
Bunch charge, nC	0.03-10.7
Pulse repetition rate, kHz	78
RMS bunch length, ps	10-500
Kinetic energy, MeV	14.5

113 MHz SRF gun with warm CsK_2Sb photocathode

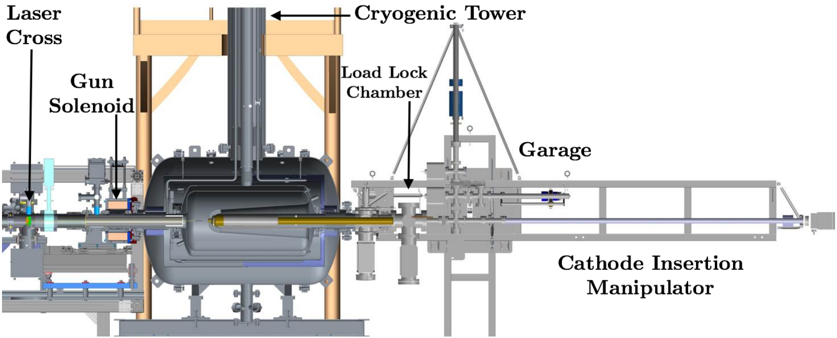

Operating temperature, K	4
CW voltage, MV	1.25
Maximal charge, nC	10.7
Normalized emittance for a 600 pC, 400 ps e-beam	
Projected emittance, mm-mrad	0.57
Slice emittance, mm-mrad	0.35

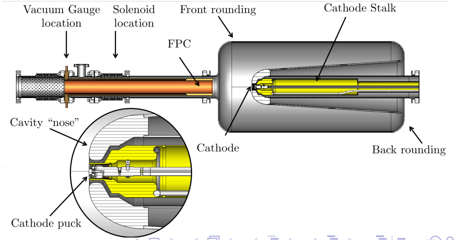

CeC PoP Accelerator Performance

Achieved parameters of the e^- beam.

Parameter	Design	Status	Comment
Species in RHIC (GeV/u)	Au^{+79} 40	Au^{+79} 26.5	to match e-beam
Electron energy (MeV)	21.95	14.56	linac quench
Charge per e-bunch (nC)	0.5-5	0.1-10.7	✓
Peak current (A)	100	50-100	✓
Bunch duration (psec)	10-50	12	✓
Normalized emittance (μm)	<5	3-5	✓
Energy spread, RMS (%)	0.1	0.1	✓
FEL wavelength (μm)	13	31	new IR diagnostics
Repetition rate (kHz)	78.18	78.18	✓
CW beam (μA)	<400	150	✓

Puzzle of the CeC Run 18

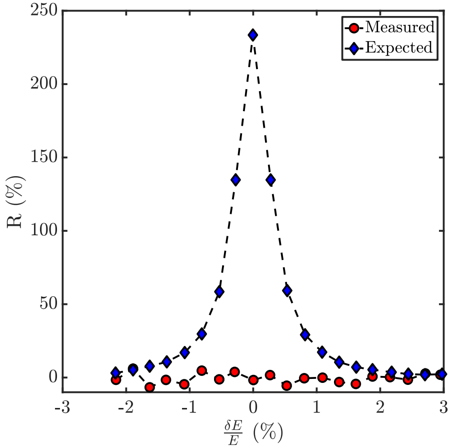

$$\boxed{R = \frac{I_{\text{overlap}} - I_{\text{separated}}}{I_{\text{separated}}}}$$

Evolution of the bunch lengths for interacting (blue trace) and witness bunches (orange and green traces).

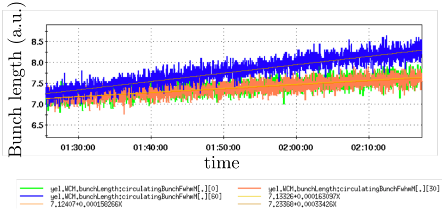

Heating of ion beam was occurring only with a perfect overlap of the beams and high FEL gain. Reducing the FEL gain eliminated the heating.

Puzzle of the CeC Run 18

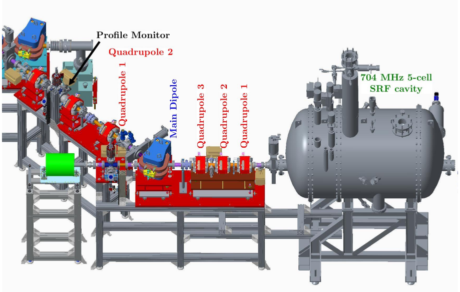

- Bunch spectra have demonstrated a broadband PCI gain peaking at ~0.4 THz in an uncompressed beam.
- Bunched beam spectrum has a peak at 10 THz.
- The measurements were confirmed through simulations done by SPACE and Impact-T.

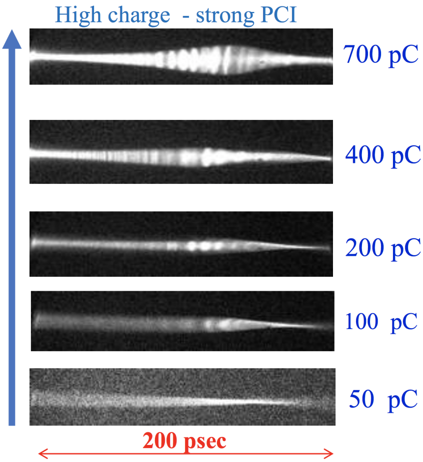

Beam profiles showing the dependence of the structures on charge per bunch.

Plasma-Cascade Instability—

longitudinal plasma oscillation with periodically varying plasma frequency:

$$\tilde{n}'' + \omega_p^2(s)\tilde{n} = 0$$

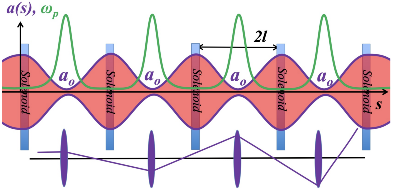

$$\boxed{\hat{a}'' - k_{\rm sc}^2\hat{a}^{-1} - k_\beta^2\hat{a}^{-3} = 0, \quad \hat{n}'' + 2k_{\rm sc}^2\hat{a}^{-2}\hat{n} = 0.}$$

$$\hat{a} = \frac{a}{a_0}, \; \hat{s} = \frac{s}{l} \in \{-1, 1\}$$

$$k_{\rm sc} = \sqrt{\frac{2}{\beta^3\gamma^3}\frac{I_0}{I_a}\frac{l^2}{a_0^2}}, \; k_\beta = \frac{\varepsilon l}{a_0^2}$$

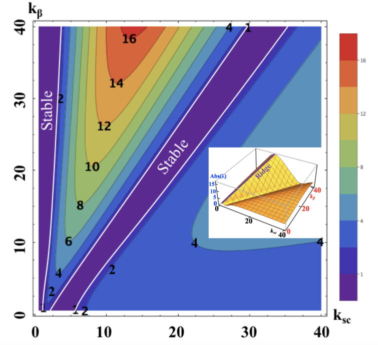

Goal of 2019

Demonstrate generation of electron beam with parameters satisfying or exceeding requirements for the CeC demonstration experiment.

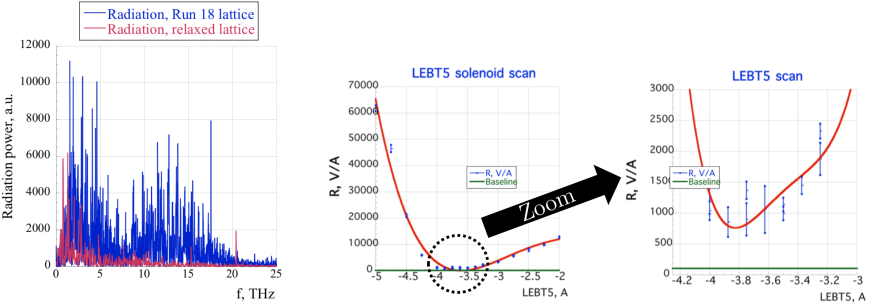

- As a result of optimization we were able to achieve the IR signal only factor two above shot noise level.
- The optimized set-up has rather flat response of the noise on the variation of the solenoid current leaving sufficient headroom for optimizing other beam parameters.

PCI applications → ACeC

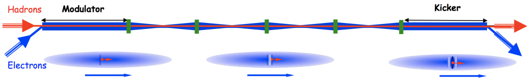

Changing CeC amplifier: FEL → PCA

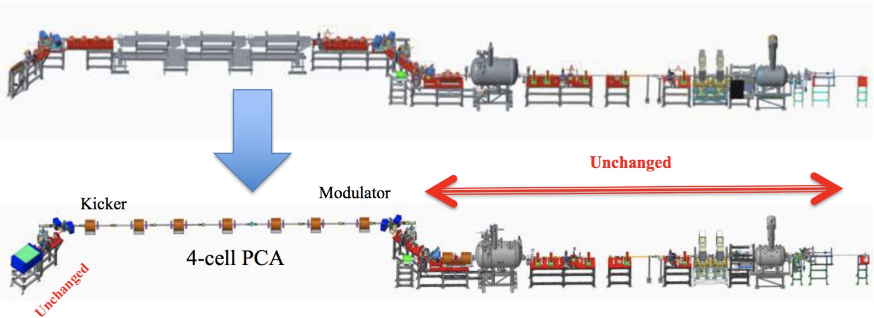

- Mechanical design of the new CeC system is completed.
- New laser system is procured and commissioned.
- All new vacuum chambers with beam diagnostics are built and installed.
- All solenoids are designed, manufactured, delivered and underwent magnetic measurements.
- Assembly of the ACeC can be completed during this year.

Conclusions

- Accelerator delivered the beam with parameters suitable for the CeC PoP experiment:
  - Normalized emittance as low as 0.35 mm-mrad for a 600 pC bunch was measured.
  - Relative energy spread 3×10^{-4} was demonstrated.
- We were unable to demonstrate the imprint of the hadrons on the electron beam due to the discovered Plasma-Cascade Instability.
- The development of the PCI was experimentally confirmed in the dedicated studies, and methods for its suppression were developed.
- The PCA-based CeC system will be tested during Runs 20-22.

Thank you for your attention!

Plasma-Cascade Instability (PCI)

Plasma-Cascade Instability

Longitudinal plasma oscillation with periodically varying plasma frequency:

$$\tilde{n}'' + \omega_p^2(s)\tilde{n} = 0$$

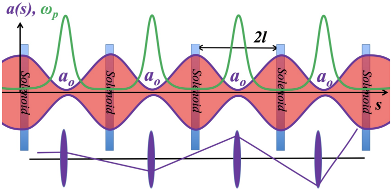

$$\boxed{\hat{a}'' - k_{\mathrm{sc}}^2 \hat{a}^{-1} - k_\beta^2 \hat{a}^{-3} = 0, \quad \hat{n}'' + 2k_{\mathrm{sc}}^2 \hat{a}^{-2}\hat{n} = 0.}$$

$$\hat{a} = \frac{a}{a_0},\ \hat{s} = \frac{s}{l} \in \{-1, 1\}$$

$$k_{\mathrm{sc}} = \sqrt{\frac{2}{\beta^3\gamma^3}\frac{I_0}{I_a}\frac{l^2}{a_0^2}},\ k_\beta = \frac{\varepsilon l}{a_0^2}$$

FODO

Betatron motion in a FODO cell:

$$y'' + K_y(s)y = 0$$

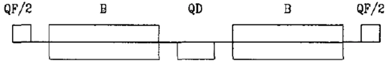

$$M = \begin{bmatrix} 1 & 0 \\ -1/2f_1 & 1 \end{bmatrix} \begin{bmatrix} 1 & L_1 \\ 0 & 1 \end{bmatrix} \begin{bmatrix} 1 & 0 \\ 1/f_2 & 1 \end{bmatrix} \begin{bmatrix} 1 & L_1 \\ 0 & 1 \end{bmatrix} \begin{bmatrix} 1 & 0 \\ -1/2f_1 & 1 \end{bmatrix} =$$

$$\begin{bmatrix} 1 + \frac{L_1}{f_2} - \frac{L_1}{f_1} - \frac{L_1^2}{f_1 f_2} & 2L_1\left(1 + \frac{L_1}{2f_2}\right) \\ \frac{1}{f_2} - \frac{1}{f_1} - \frac{L_1}{f_1 f_2} + \frac{L_1^2}{2f_1^2} + \frac{L_1^2}{4f_1^2 f_2} & 1 + \frac{L_1}{f_2} - \frac{L_1}{f_1} - \frac{L_1^2}{f_1 f_2} \end{bmatrix}$$

CeC schemes

Litvinenko, Derbenev, PRL 2008

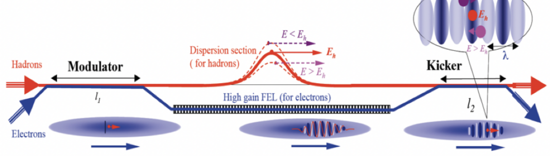

High gain FEL amplifier

Ratner, PRL 2013

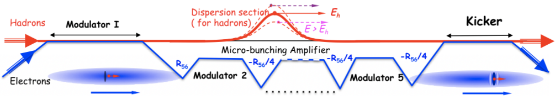

Multi- Chicane Microbunching amplifier

Litvinenko, Wang, Kayran, Jing, Ma, 2017

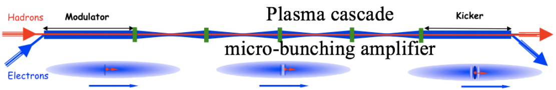

Plasma-Cascade Microbunching amplifier

Litvinenko, Cool 13

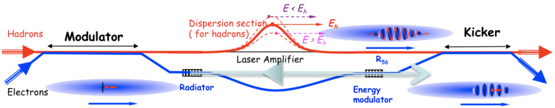

Hybrid laser-beam amplifier

Advantages and Disadvantages

- The best studied and fully explored scheme
- Experimentally demonstrated both as instability and amplifier
- 3D FEL theory and simulation are very advanced
- Can operate at relatively low electron beam peak currents
- Allows – in principle – economic option without separating electron and hadron beams

- When compared with micro-bunching amplifier, it has relatively lower bandwidth ~ few % of the FEL frequency
- FEL saturates at lower gain than micro-bunching amplifier
- Semi-periodic structure of the modulation limits the range where cooling occurs

CeC with High gain FEL amplifier

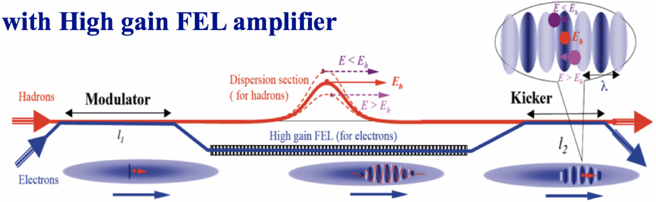

Stony Brook University

Advantages and Disadvantages

- Very broad band amplifier, can operate at significant gain without saturation
- Plasma-cascade micro-bunching instability was experimentally demonstrated
- Has good theoretical model and is extensively studied in 3D numerical simulations
- Cool hadrons with all energy deviation (no anti-cooling)
- Does not require (full) separation of electron and hadron beams

- Micro-bunching amplifier was not demonstrated
- Requires better quality electron beam than FEL amplifier
- Can operate for medium hadron energies (up to hundreds of GeV, such as US EIC), but can not be extended to LHC energies
- Less studied than FEL-based CeC

Plasma-Cascade Microbunching amplifier

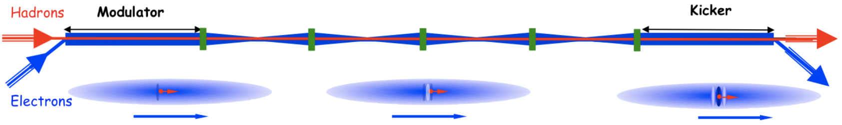

Stony Brook University

What is cooling and why do we need it?

Luminosity characterizes the ability of a particle accelerator to produce the required number of interactions:

$$\frac{dN}{dt} = \sigma \cdot L \tag{1}$$

$$L = \frac{N_1 \times N_2 \times frequency}{Overlap\ Area} = \frac{N_1 \times N_2 \times f_{coll}}{4\pi\beta^*\varepsilon} \times h\left(\frac{\sigma_s}{\beta^*}\right) \tag{2}$$

We want to have a large charge per bunch, high collision frequency and small spot size!

Cooling:

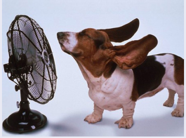

reduces beam phase space volume, emittance and momentum spread in order to improve beam quality.

Coherent electron Cooling (CeC)

CeC scheme is based on electrostatic interactions between electrons and hadrons that are amplified either in a high-gain FEL or by other means.

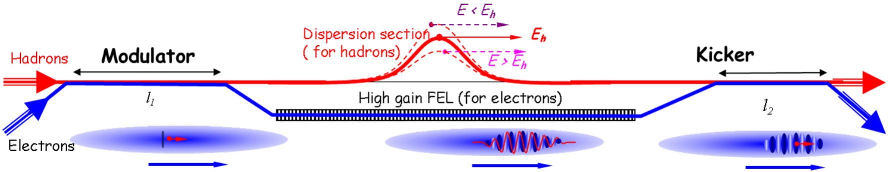

The electron and hadron beams co-propagate in a vacuum along a straight line in the modulator and kicker with the same velocity:

$$\gamma = \frac{E_e}{m_e c^2} = \frac{E_h}{m_h c^2} \tag{3}$$

Coherent electron Cooling (CeC): Kicker

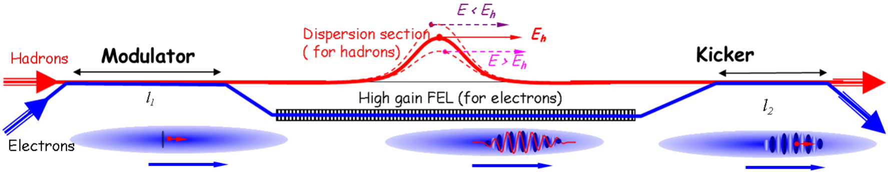

- When the hadron and electron beams are recombined, hadrons are exposed to the longitudinal electric field
- With a proper delay section, a hadron with central energy E_0 arrives at the kicker on top of the electron density peak—zero electric field
- Hadrons with higher energy are decelerated, and ones with lower energy are pulled forward.

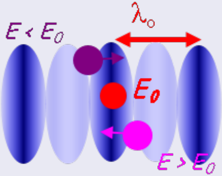

Coherent electron Cooling: Proof of Principle

Parameter	Value
Gun energy, MeV	1.25
Beam charge, nC	1-5
Final beam energy, MeV	14.6
Normalized emittance, mm-mrad	<5
Energy spread	10^{-3}
Pulse repetition rate, kHz	78

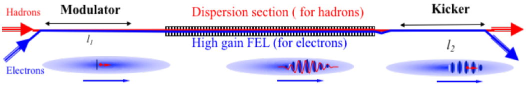

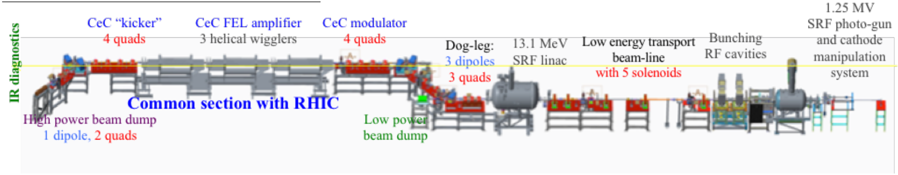

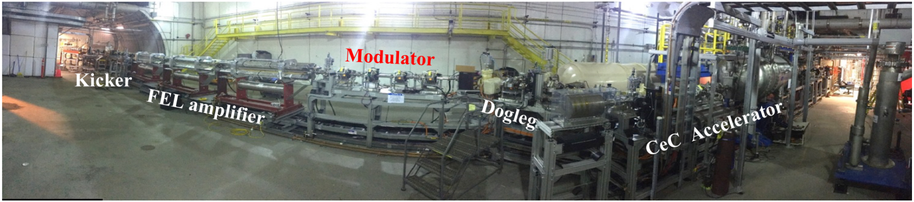

Coherent electron Cooling: Proof of Principle

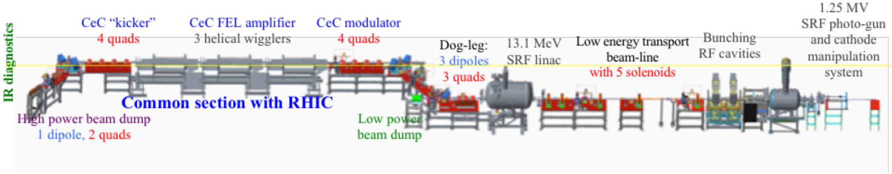

- e^- beam is generated by 113 MHz SRF gun with CsK_2Sb photocathode driven by a 532 nm laser
- Two 500 MHz copper cavities provide energy chirp and beam is compressed to desired peak current.
- After the compression beam is accelerated by a 704 MHz SRF cavity and merged into CeC PoP structure with three helical undulators.

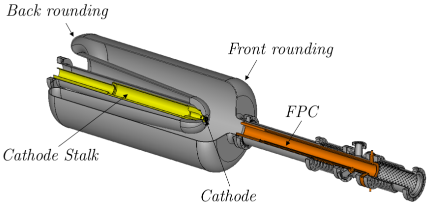

Coherent electron Cooling: Proof of Principle

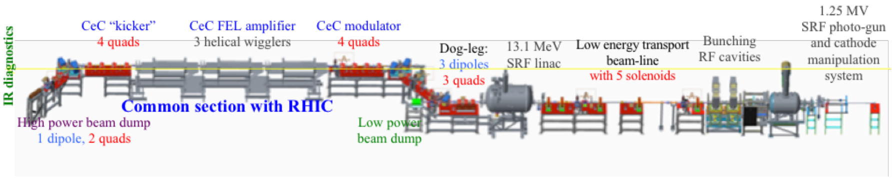

- e^- beam is generated by 113 MHz SRF gun with CsK_2Sb photocathode driven by a 532 nm laser
- Two 500 MHz copper cavities provide energy chirp and beam is compressed to desired peak current.
- After the compression beam is accelerated by a 704 MHz SRF cavity and merged into CeC PoP structure with three helical undulators.

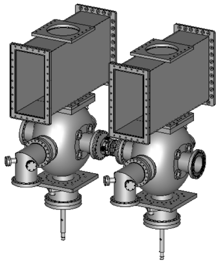

Coherent electron Cooling: Proof of Principle

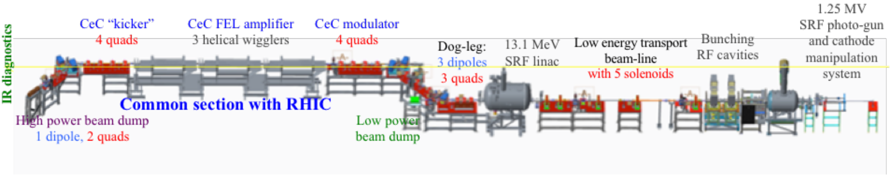

- e^- beam is generated by 113 MHz SRF gun with CsK_2Sb photocathode driven by a 532 nm laser
- Two 500 MHz copper cavities provide energy chirp and beam is compressed to desired peak current.
- After the compression beam is accelerated by a 704 MHz SRF cavity and merged into CeC PoP structure with three helical undulators.

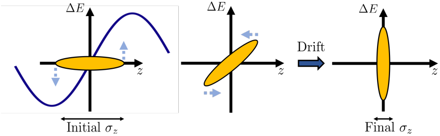

Coherent electron Cooling: Proof of Principle

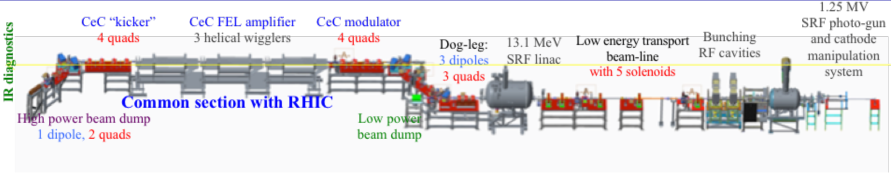

- e^- beam is generated by 113 MHz SRF gun with CsK_2Sb photocathode driven by a 532 nm laser
- Two 500 MHz copper cavities provide energy chirp and beam is compressed to desired peak current.
- After the compression beam is accelerated by a 704 MHz SRF cavity and merged into CeC PoP structure with three helical undulators.

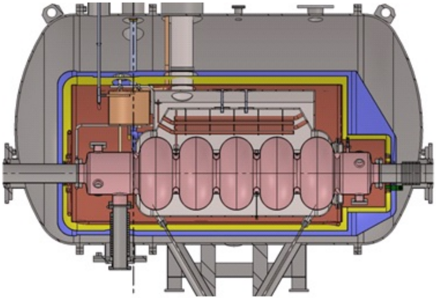

Pros:

- Good vacuum inside Nb cavity at 2K/4K
- Relatively high accelerating gradients
- CW operation

Cons/Questions:

- Are high-QE cathodes compatible with SRF?
- Can high-QE cathodes survive in an SRF cavity?
- How to keep cathodes at room temperature without causing multipacting (MP)?
- How to get to operational voltage without causing MP and killing cathode?
- Dark current?

It is expensive and challenging—hence,
there are very few operational SRF guns!

Overview of existing SRF photoinjectors

Parameter	CeC PoP	FZD[1]	HZB[2]	NPS[3]	UW[4]
Cavity type	QWR*	Elliptical	Elliptical	QWR	QWR
Number of cells	1	3.5	1.4	1	1
RF frequency, MHz	113	1300	1300	500	200
LiHe Temperature, K	4	2	2	4	4
Beam energy, MeV	1.25-1.5	3.3	1.8	0.47	1.1
Charge per bunch, nC	10.7	0.3	0.006	0.078	0.1
Beam current, μA	150	18	0.005	<0.0001	<0.1
Dark current, nA	<1	120	-	<20, 000	<0.001
E_{cath}, MV/m	10-20	5	7	6.5	12
Photocathode	CsK_2Sb	Cs_2Te	Pb	Ni	Cu

*QWR—Quarter Wave Resonator

[1] A. Arnold et al. "A high-brightness SRF photoelectron injector for FEL light sources". In: *Nuclear Instruments and Methods in Physics Research Section A: Accelerators, Spectrometers, Detectors and Associated Equipment* 593.1 (2008), pp. 57–62.

[2] M. Schmeißer et al. "Results from beam commissioning of an SRF plug-gun cavity photoinjector". In: (2013).

[3] J.R. Harris et al. "Design and operation of a superconducting quarter-wave electron gun". In: *Physical Review Special Topics-Accelerators and Beams* 14.5 (2011), p. 053501.

[4] J. Bisognano et al. "Wisconsin SRF Electron Gun Commissioning". In: *Proc. NAPAC'13* (2013), pp. 622–624.

CeC PoP SRF gun with warm CsK_2Sb photocathode

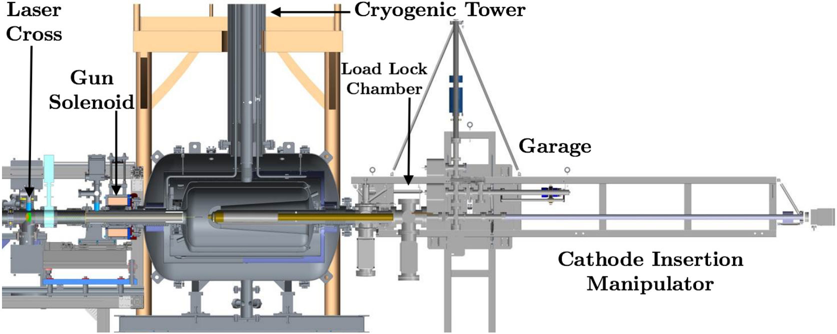

- Quarter-wave cavity.
- 4 K operating temperature.
- 4 kW CW solid state power amplifier.
- CsK_2Sb cathode is at room temperature.
- Up to three cathodes can be stored in garage for quick exchange.
- Design gradient 22.5 MV/m.

113 MHz SRF Photo-Injector: Performance

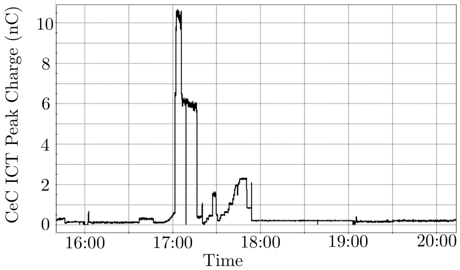

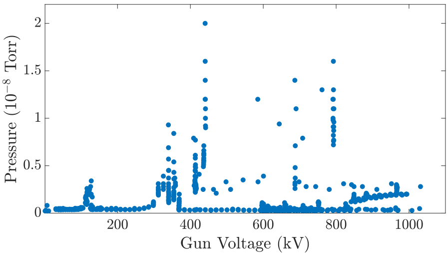

- The gun can generate electron bunches with charge per bunch exceeding 10 nC (saturated the diagnostics).
- During the first years of operation the gun was affected by multipacting.

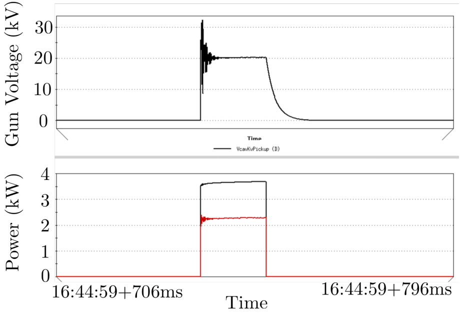

Definition of multipacting

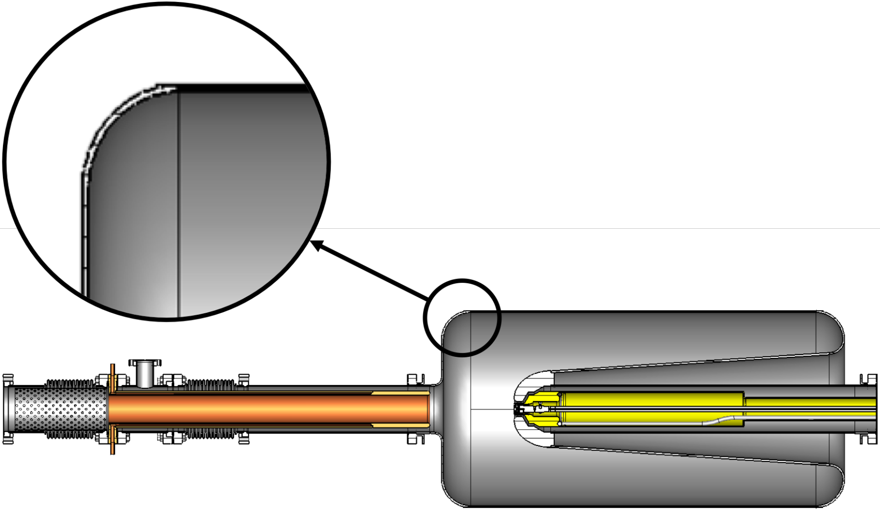

Definition of multipacting

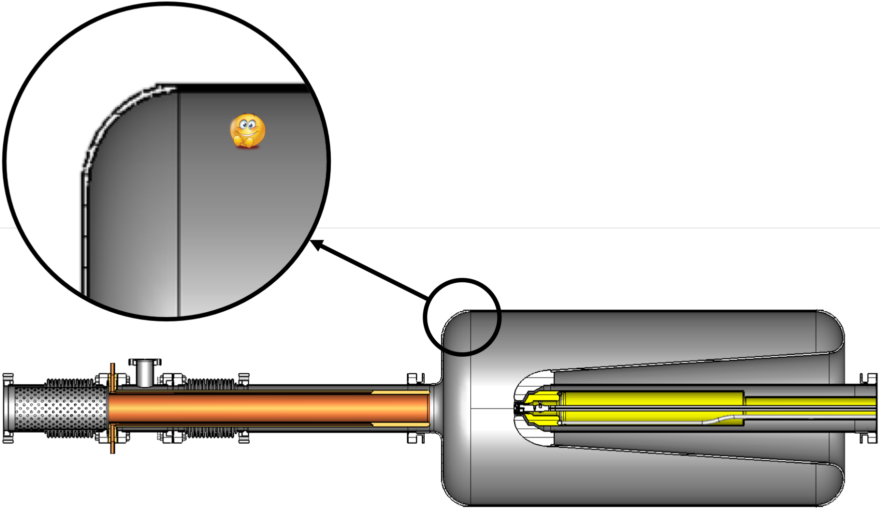

Definition of multipacting

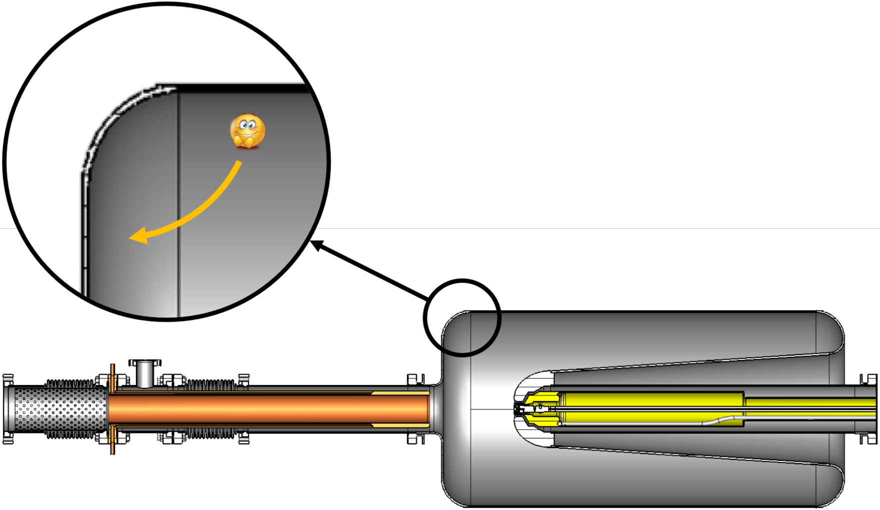

Definition of multipacting

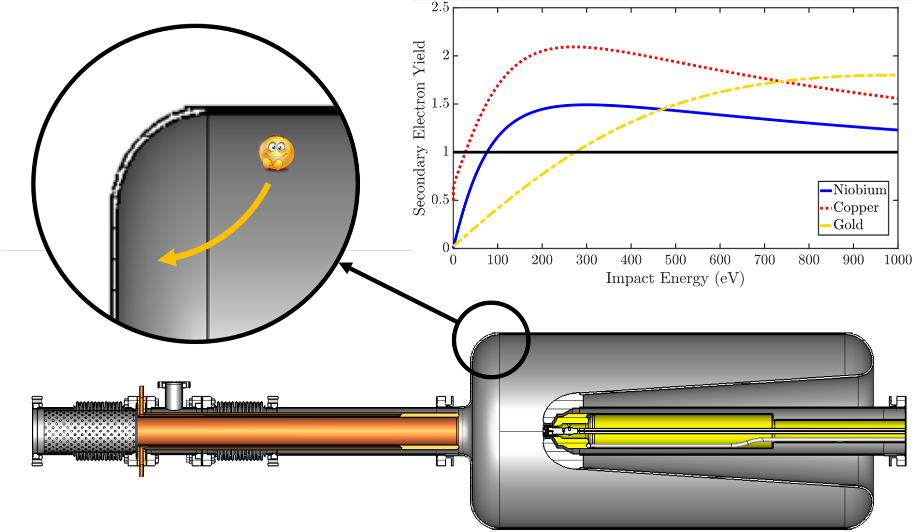

Definition of multipacting

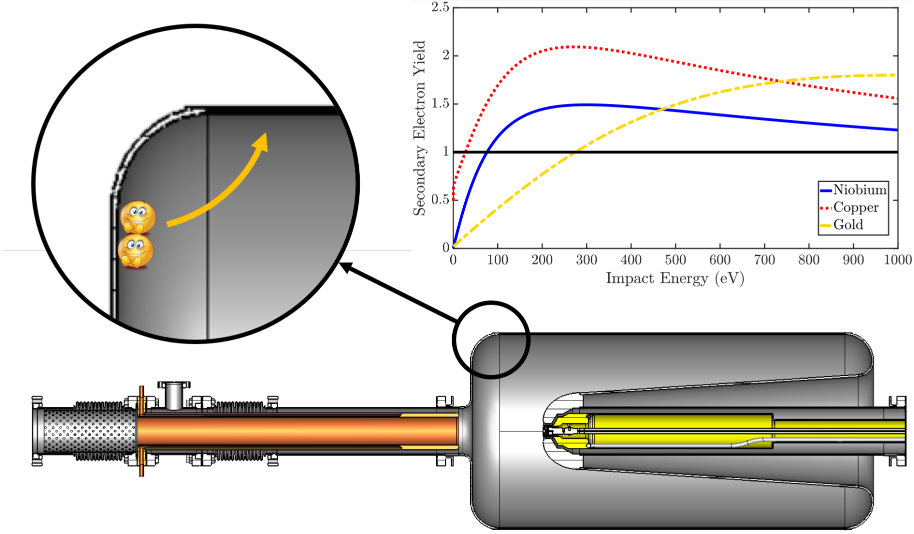

Definition of multipacting

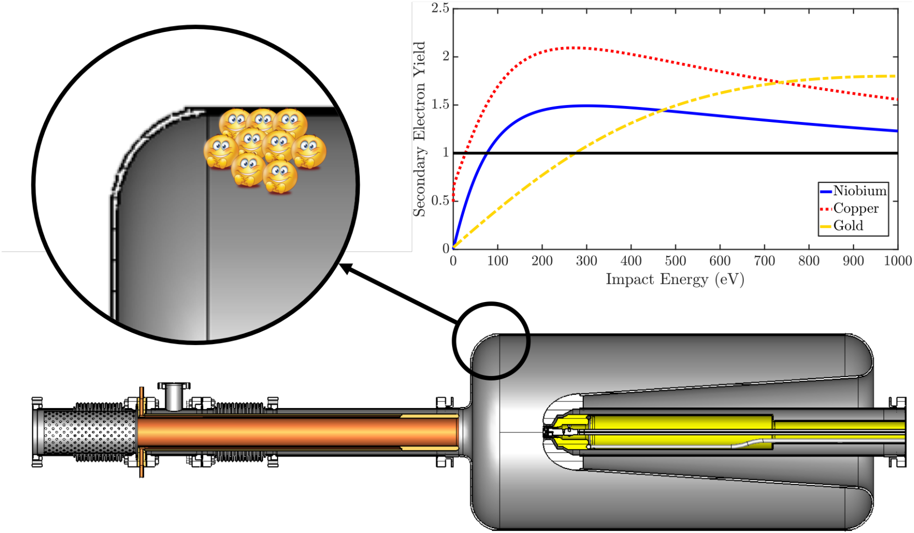

MP Simulations: Affected Areas & Influence of B-Field

CST Particle Studio

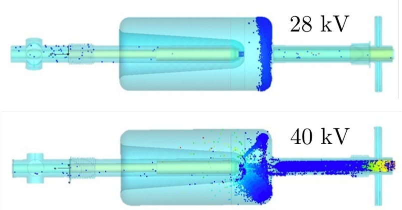

ACE3P (Track3P)

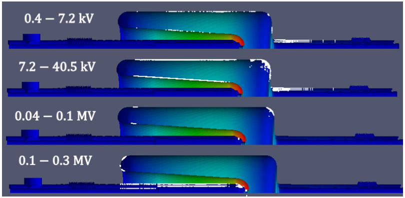

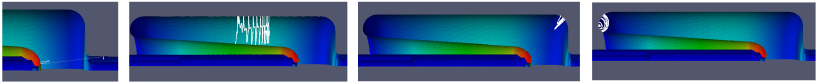

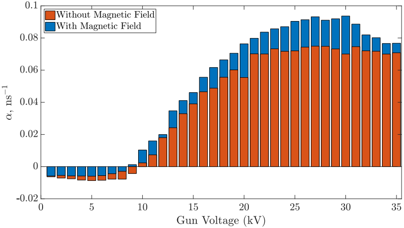

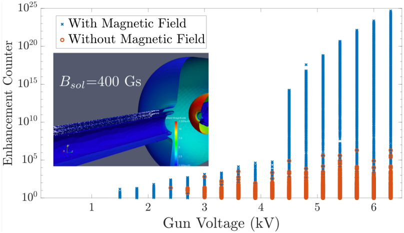

Multipacting Well Studied and Understood Now

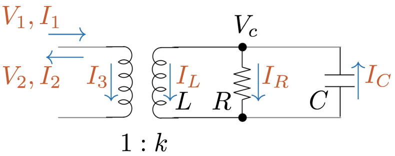

$$\begin{cases} \dfrac{d|V_c|}{dt} = \frac{1}{2\tau}\left(|V_0| - |V_c|\right) - f_0 \delta V_{mp} \dfrac{eN_e(t)}{2Q_0|V_c|}\omega_0 R_{sh}, \\ \dfrac{dN_e}{dt} = \alpha(|V_c|)N_e. \end{cases}$$

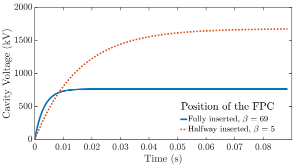

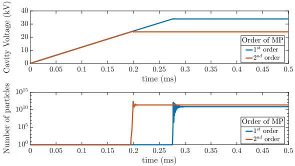

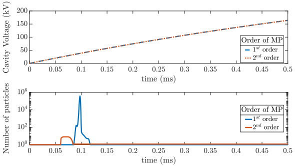

PHYSICAL REVIEW ACCELERATORS AND BEAMS **21,** 082001 (2018)

Mitigation of multipacting in 113 MHz superconducting rf photoinjector

I. Petrushina,[1,2,*] V. N. Litvinenko,[1,2] I. Pinayev,[2] K. Smith,[2] G. Narayan,[2] and F. Severino[2]
[1]*Department of Physics and Astronomy, Stony Brook University, Stony Brook, New York 11794, USA*
[2]*Collider-Accelerator Department, Brookhaven National Laboratory, Upton, New York 11973, USA*

(Received 28 February 2018; published 13 August 2018)

Example of Cavity Turn On Attempt with Strong MP

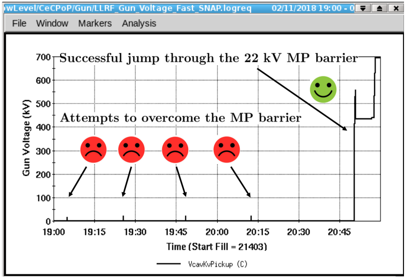

- Four repeated attempts to turn on result in getting stuck at 22 kV MP barrier.
- Attempts last only 20 ms, controlled by LLRF MP trap code.
- Prevents significant energy deposition $\Rightarrow$ vacuum activity which would kill cathode QE.

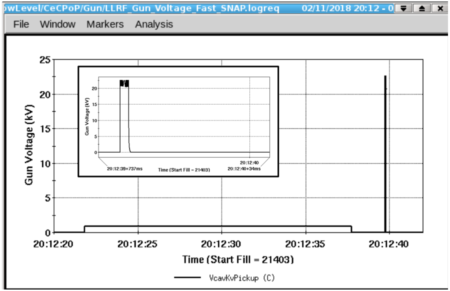

- Lengthen period between attempts from $\sim$ 20 min to $\sim$ 40 min $\Rightarrow$ 5^{th} attempt = successful turn on.
- Cathode QE not impacted by turn on attempts as MP related vacuum activity is kept minimal.

Challenges of the beam dynamics simulations in the gun

- Traditional simulations tools (PARMELA, GPT, ASTRA, BMAD, IMPACT-T) have a difficulty to properly simulate beam dynamics inside the SRF gun.
- There is no problem to perform simulations outside of the gun, but the challenge is in grasping the details of the environment in the cathode vicinity.
- **Goal: utilize Particle In Cell (PIC) codes dedicated to such problems, and use the resulting distribution in the start-to-end simulations.**

Particle In Cell (PIC): algorithm & the PIC codes

The equations of motion used for the simulations:

$$\frac{d\vec{r}}{dt} = \frac{\vec{p}}{m\gamma}; \; \frac{d\vec{p}}{dt} = q\left(\vec{E} + \frac{\vec{p}}{m\gamma} \times \vec{B}\right).$$

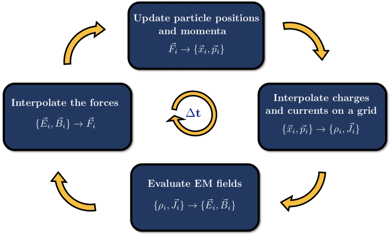

Parameter	**CST PS**	**Pic3P**	**GPT**	**IMPACT-T**
		Specifics of the algorithm		
Equations solved	Maxwell	Maxwell	Poisson	Poisson
Wakefileds	✓	✓	×	×
Space charge	✓	✓	✓	✓
Retardation effects	✓	✓	×	×
Image charge	Real geometry	Real geometry	Flat wall	Flat wall
		Simulation setup		
Field distribution	CST MWS	Omega3P	SUPERFISH (map)	SUPERFISH (E_z)
Transverse particle distribution	Area/Circular		Uniform	Uniform
Longitudinal particle distribution	Truncated Gaussian	Uniform	Uniform	Uniform
		Performance		
Computational resources	Intel Core i7 (8 CPU)	NERSC	Intel Core i7 (8 CPU)	Intel Core i7 (8 CPU)
Duration	1 week	1 day	1 day	5 hours

Comparison with the experiment

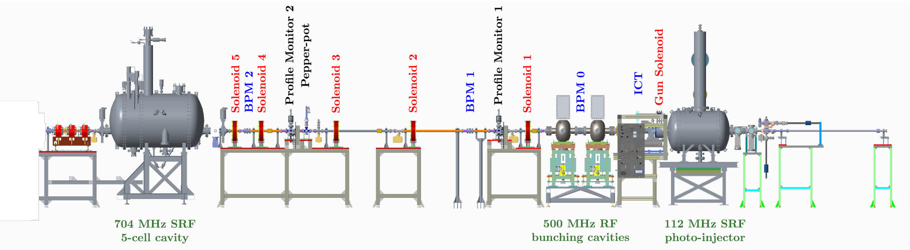

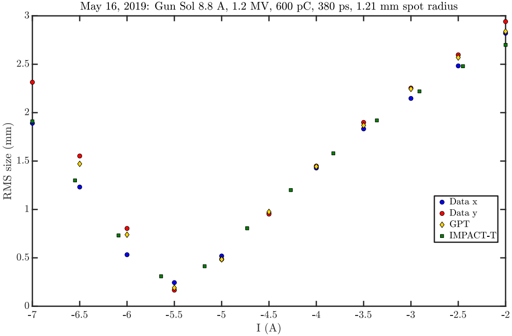

- Turn off the bunching cavities
- Scan LEBT 1 solenoid at a fixed value of the gun solenoid
- Measure the RMS beam size at YAG 1.

Emittance, what is it?

Emittance, ε:

measure of the area A occupied by a beam in phase space.

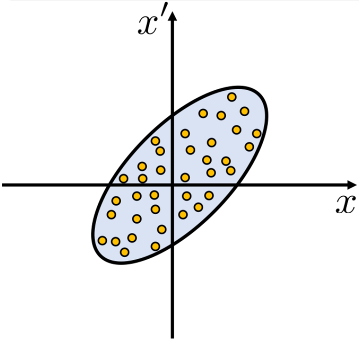

$$\varepsilon = \sqrt{\langle x^2 \rangle \langle x'^2 \rangle - \langle x x' \rangle^2}, \text{ with}$$

$$\langle x^2 \rangle = \sigma_x^2 = \frac{1}{N} \sum_{i=1}^{N} (x_i - \langle x \rangle)^2,$$

$$\langle x'^2 \rangle = \sigma_{x'}^2 = \frac{1}{N} \sum_{i=1}^{N} (x'_i - \langle x' \rangle)^2,$$

$$\langle x x' \rangle = \sigma_{xx'} = \frac{1}{N} \sum_{i=1}^{N} (x_i - \langle x \rangle)(x'_i - \langle x' \rangle).$$

Normalized emittance, ε_n:

$$\varepsilon_n = \varepsilon \gamma \beta,$$

with relativistic parameters β and γ defined by the energy of the beam.

Slice emittance & Emittance compensation

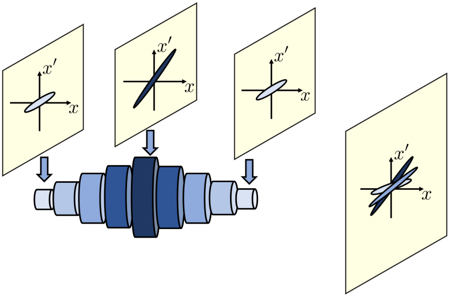

- Slices have different emittance and ellipse orientation;
- Variation in the ellipse orientation leads to a high projected emittance;
- Projected emittance can be reduced by the alignment of the slices.

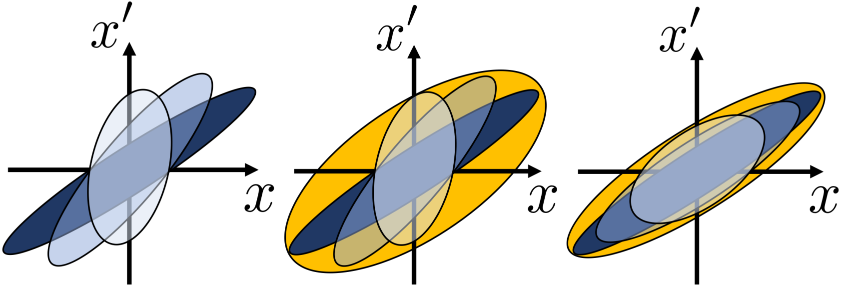

How to measure emittance

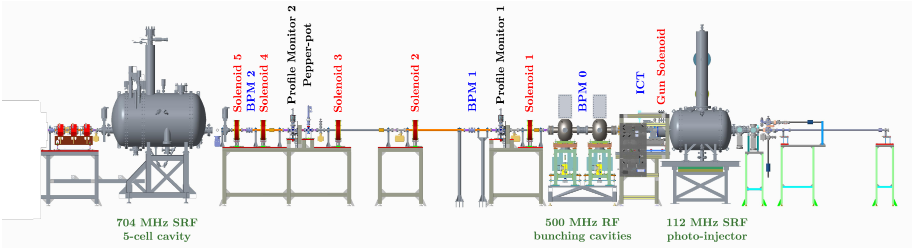

Matrix of a solenoid:

$$F = \begin{pmatrix} 1 & 0 \\ 1/f_{\mathrm{sol}} & 1 \end{pmatrix}, \; 1/f_{\mathrm{sol}} = \int \left(\frac{eB_s}{2pc}\right)^2 ds$$

Solenoid+drift:

$$M = \begin{pmatrix} 1 & L \\ 0 & 1 \end{pmatrix} \begin{pmatrix} 1 & 0 \\ 1/f_{\mathrm{sol}} & 1 \end{pmatrix} = \begin{pmatrix} m_{11} & m_{12} \\ m_{21} & m_{22} \end{pmatrix}$$

Beam matrix:

$$\Sigma_{\mathrm{beam}} = \begin{pmatrix} \sigma_x^2 & \sigma_{xx'} \\ \sigma_{xx'} & \sigma_{x'}^2 \end{pmatrix}$$

$$\sigma_b^2 = m_{11}^2\sigma_x^2 + 2m_{11}m_{12}\sigma_{xx'} + m_{12}^2\sigma_{x'}^2$$

$$\sigma_b^2 = \varepsilon(m_{11}^2\beta_0 - 2m_{11}m_{12}\alpha_0 + m_{12}^2\frac{1+\alpha_0^2}{\beta_0})$$

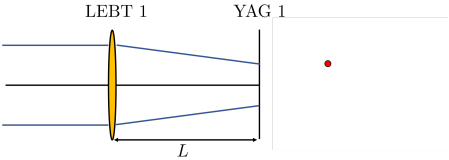

How to measure emittance

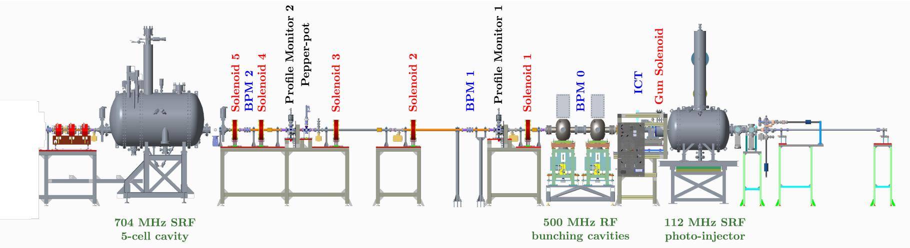

Matrix of a solenoid:

$$F = \begin{pmatrix} 1 & 0 \\ 1/f_{\mathrm{sol}} & 1 \end{pmatrix}, \; 1/f_{\mathrm{sol}} = \int \left(\frac{eB_s}{2pc}\right)^2 ds$$

Solenoid+drift:

$$M = \begin{pmatrix} 1 & L \\ 0 & 1 \end{pmatrix} \begin{pmatrix} 1 & 0 \\ 1/f_{\mathrm{sol}} & 1 \end{pmatrix} = \begin{pmatrix} m_{11} & m_{12} \\ m_{21} & m_{22} \end{pmatrix}$$

Beam matrix:

$$\Sigma_{\mathrm{beam}} = \begin{pmatrix} \sigma_x^2 & \sigma_{xx'} \\ \sigma_{xx'} & \sigma_{x'}^2 \end{pmatrix}$$

$$\sigma_b^2 = m_{11}^2 \sigma_x^2 + 2 m_{11} m_{12} \sigma_{xx'} + m_{12}^2 \sigma_{x'}^2$$

$$\sigma_b^2 = \varepsilon (m_{11}^2 \beta_0 - 2 m_{11} m_{12} \alpha_0 + m_{12}^2 \frac{1+\alpha_0^2}{\beta_0})$$

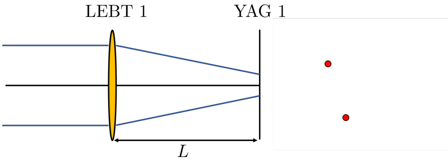

How to measure emittance

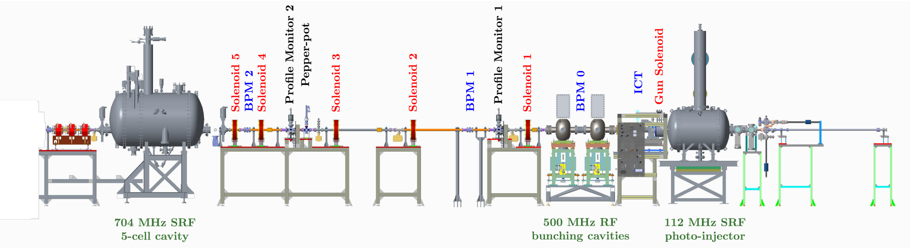

Matrix of a solenoid:

$$F = \begin{pmatrix} 1 & 0 \\ 1/f_{\mathrm{sol}} & 1 \end{pmatrix},\ 1/f_{\mathrm{sol}} = \int \left(\frac{eB_s}{2pc}\right)^2 ds$$

Solenoid+drift:

$$M = \begin{pmatrix} 1 & L \\ 0 & 1 \end{pmatrix} \begin{pmatrix} 1 & 0 \\ 1/f_{\mathrm{sol}} & 1 \end{pmatrix} = \begin{pmatrix} m_{11} & m_{12} \\ m_{21} & m_{22} \end{pmatrix}$$

Beam matrix:

$$\Sigma_{\mathrm{beam}} = \begin{pmatrix} \sigma_x^2 & \sigma_{xx'} \\ \sigma_{xx'} & \sigma_{x'}^2 \end{pmatrix}$$

$$\sigma_b^2 = m_{11}^2 \sigma_x^2 + 2m_{11}m_{12}\sigma_{xx'} + m_{12}^2 \sigma_{x'}^2$$

$$\sigma_b^2 = \varepsilon(m_{11}^2 \beta_0 - 2m_{11}m_{12}\alpha_0 + m_{12}^2 \frac{1+\alpha_0^2}{\beta_0})$$

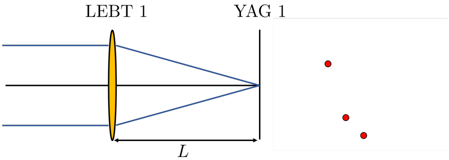

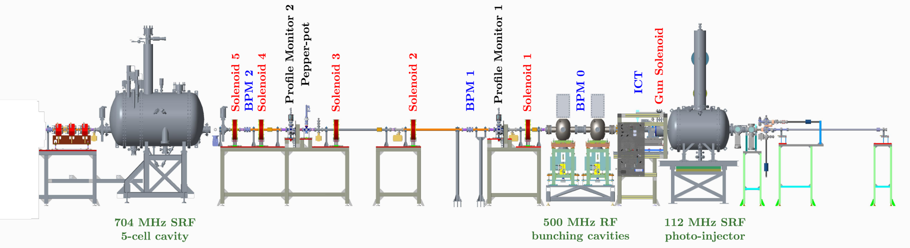

Matrix of a solenoid:

$$F = \begin{pmatrix} 1 & 0 \\ 1/f_{\rm sol} & 1 \end{pmatrix},\ 1/f_{\rm sol} = \int \left(\frac{eB_s}{2pc}\right)^2 ds$$

Solenoid+drift:

$$M = \begin{pmatrix} 1 & L \\ 0 & 1 \end{pmatrix} \begin{pmatrix} 1 & 0 \\ 1/f_{\rm sol} & 1 \end{pmatrix} = \begin{pmatrix} m_{11} & m_{12} \\ m_{21} & m_{22} \end{pmatrix}$$

Beam matrix:

$$\Sigma_{\rm beam} = \begin{pmatrix} \sigma_x^2 & \sigma_{xx'} \\ \sigma_{xx'} & \sigma_{x'}^2 \end{pmatrix}$$

$$\sigma_b^2 = m_{11}^2\sigma_x^2 + 2m_{11}m_{12}\sigma_{xx'} + m_{12}^2\sigma_{x'}^2$$

$$\sigma_b^2 = \varepsilon(m_{11}^2\beta_0 - 2m_{11}m_{12}\alpha_0 + m_{12}^2\frac{1+\alpha_0^2}{\beta_0})$$

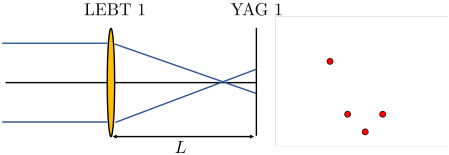

How to measure emittance

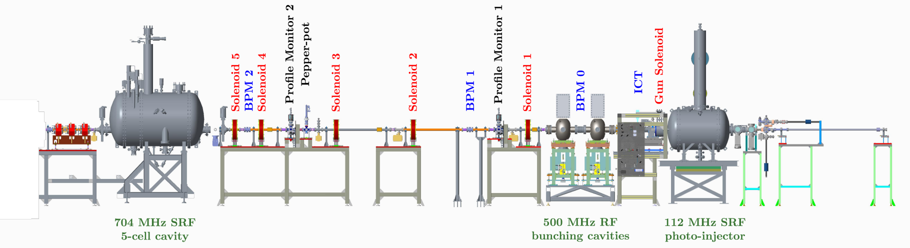

Matrix of a solenoid:

$$F = \begin{pmatrix} 1 & 0 \\ 1/f_{\text{sol}} & 1 \end{pmatrix}, \; 1/f_{\text{sol}} = \int \left(\frac{eB_s}{2pc}\right)^2 ds$$

Solenoid+drift:

$$M = \begin{pmatrix} 1 & L \\ 0 & 1 \end{pmatrix} \begin{pmatrix} 1 & 0 \\ 1/f_{\text{sol}} & 1 \end{pmatrix} = \begin{pmatrix} m_{11} & m_{12} \\ m_{21} & m_{22} \end{pmatrix}$$

Beam matrix:

$$\Sigma_{\text{beam}} = \begin{pmatrix} \sigma_x^2 & \sigma_{xx'} \\ \sigma_{xx'} & \sigma_{x'}^2 \end{pmatrix}$$

$$\sigma_b^2 = m_{11}^2 \sigma_x^2 + 2m_{11}m_{12}\sigma_{xx'} + m_{12}^2\sigma_{x'}^2$$

$$\sigma_b^2 = \varepsilon(m_{11}^2\beta_0 - 2m_{11}m_{12}\alpha_0 + m_{12}^2\frac{1+\alpha_0^2}{\beta_0})$$

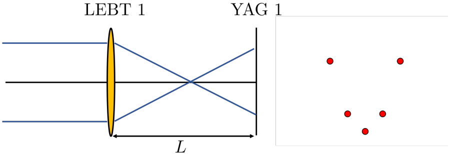

How to measure emittance

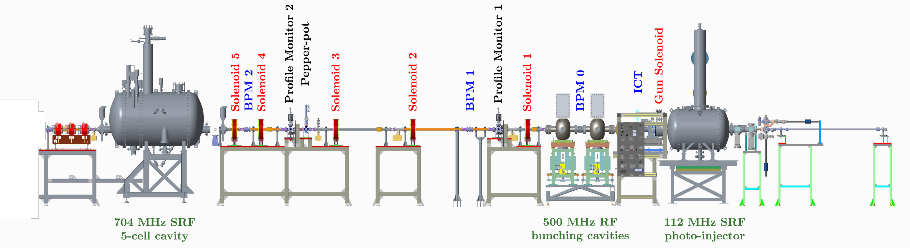

Matrix of a solenoid:

$$F = \begin{pmatrix} 1 & 0 \\ 1/f_{\text{sol}} & 1 \end{pmatrix}, \; 1/f_{\text{sol}} = \int \left(\frac{eB_s}{2pc} \right)^2 ds$$

Solenoid+drift:

$$M = \begin{pmatrix} 1 & L \\ 0 & 1 \end{pmatrix} \begin{pmatrix} 1 & 0 \\ 1/f_{\text{sol}} & 1 \end{pmatrix} = \begin{pmatrix} m_{11} & m_{12} \\ m_{21} & m_{22} \end{pmatrix}$$

Beam matrix:

$$\Sigma_{\text{beam}} = \begin{pmatrix} \sigma_x^2 & \sigma_{xx'} \\ \sigma_{xx'} & \sigma_{x'}^2 \end{pmatrix}$$

$$\sigma_b^2 = m_{11}^2 \sigma_x^2 + 2 m_{11} m_{12} \sigma_{xx'} + m_{12}^2 \sigma_{x'}^2$$

$$\sigma_b^2 = \varepsilon (m_{11}^2 \beta_0 - 2 m_{11} m_{12} \alpha_0 + m_{12}^2 \frac{1+\alpha_0^2}{\beta_0})$$

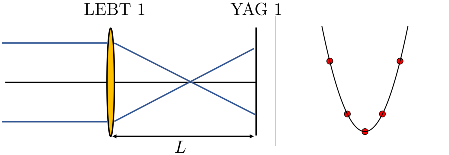

Emittance measurements

For a 100 pC e-beam we can achieve a core slice emittance as low as 0.15 mm-mrad

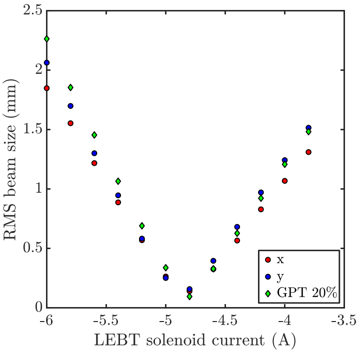

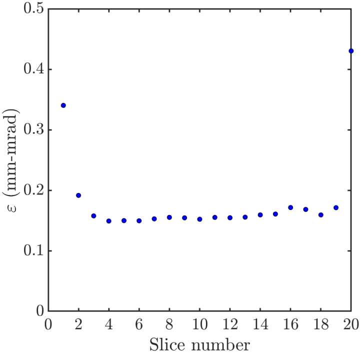

The best normalized RMS emittance achieved for 600 pC was 0.57 mm-mrad with core slice emittance of 0.35 mm-mrad.

Emittance Measurements

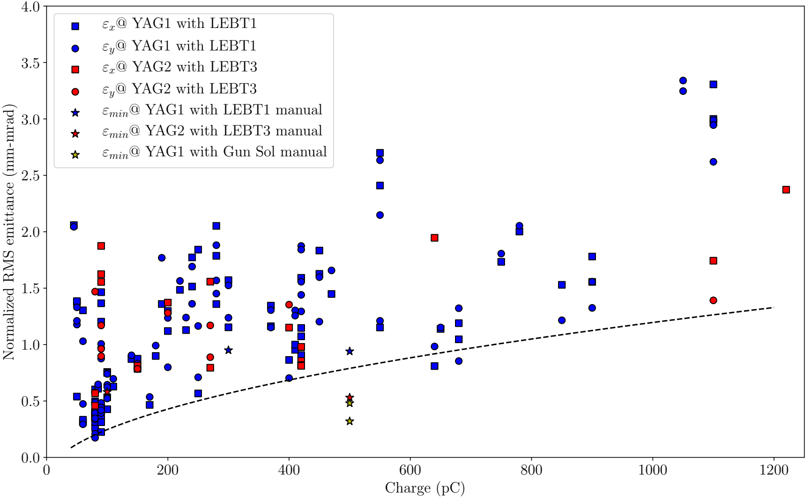

What did we learn about our photoinjector?

- We have demonstrated the record parameters for the SRF CW gun both in charge per bunch and transverse emittance.
- Photocathode at room temperature have high QE.
- Low frequency of the gun allows to generate electron beam close to conditions in a DC gun and fully utilize available field gradient.
- Good vacuum inside SRF gun provides long lifetime for the cathode.
- Multipacting is no longer a challenge.

CeC PoP Accelerator Performance

Achieved parameters of the e^- beam.

Parameter	Design	Status	Comment
Species in RHIC (GeV/u)	Au^{+79} 40	Au^{+79} 26.5	to match e-beam
Electron energy (MeV)	21.95	14.56	linac quench
Charge per e-bunch (nC)	0.5-5	0.1-10.7	✓
Peak current (A)	100	50-100	✓
Bunch duration (psec)	10-50	12	✓
Normalized emittance (μm)	<5	3-5	✓
Energy spread, RMS (%)	0.1	0.1	✓
FEL wavelength (μm)	13	31	new IR diagnostics
Repetition rate (kHz)	78.18	78.18	✓
CW beam (μA)	<400	150	✓

Plan for the CeC PoP demonstration experiment:

1. Establish the required transverse overlap of the electron and ion beams.
2. Synchronize the electron and ion beams to achieve longitudinal overlap.
3. Confirm the interaction of the beams in the modulator by measuring the FEL power.
4. Adjust the energy of the electron beam to match the ion beam energy based on the FEL signal.
5. Establish interaction between the bunches and observe the ion beam evolution in time to test the CeC.

Confirm interaction of the beams in the modulator

Indicator of the ion and electron beam interactions in the modulator section is a significant increase in the FEL power.

$$R = \frac{I_{overlap} - I_{separated}}{I_{separated}}$$

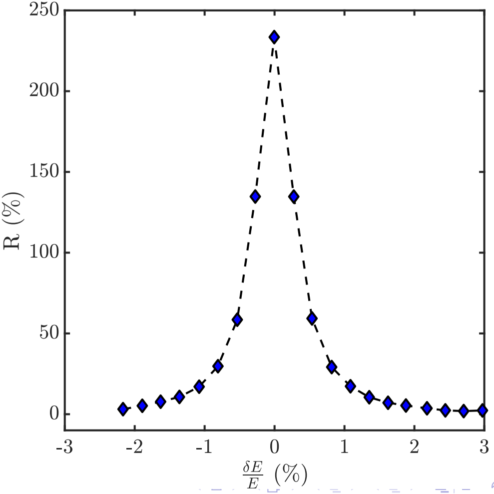

Confirm interaction of the beams in the modulator

Indicator of the ion and electron beam interactions in the modulator section is a significant increase in the FEL power.

$$R = \frac{I_{overlap} - I_{separated}}{I_{separated}}$$

?

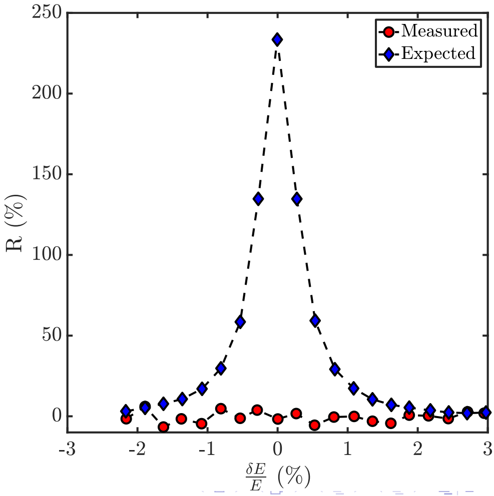

Possible reasons to investigate

1. Energy difference between the ion and electron beams was larger than 3%.
2. Transverse overlap between the bunches was reduced and therefore was insufficient for the interaction.
3. FEL was operating in saturation.
4. High initial noise level in the electron beam was present.

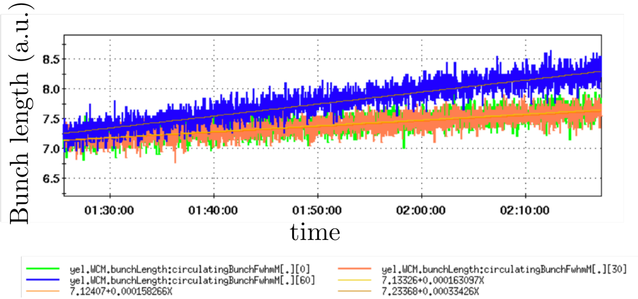

Possible reasons to investigate

1. Energy difference between the ion and electron beams was larger than 3%.

The measurements of the energy were repeated independently:

- Energy of the electron beam was reported as requested for the experiment with a $\pm 1\%$ relative error;
- Energy measurement of the ion beam in RHIC was performed with a $\pm 0.1\%$ accuracy;
- The energy difference between the beams could not be larger than $\pm 1\%$;
- The ion imprint experiment was performed in a wide ($\pm 2.5\%$) range of energies.

Possible reasons to investigate

1. ~~Energy difference between the ion and electron beams was larger than 3%.~~
2. Transverse overlap between the bunches was reduced and therefore was insufficient for the interaction.
3. FEL was operating in saturation.
4. High initial noise level in the electron beam was present.

Possible reasons to investigate: slice emittance

2. Transverse overlap between the bunches was reduced and therefore was insufficient for the interaction.

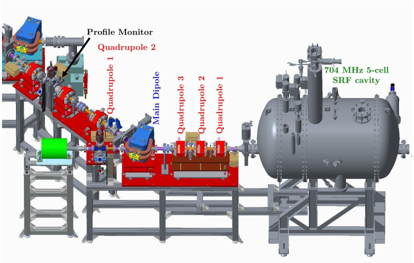

- Operate the 704 MHz cavity $\sim 15^\circ$ off-crest;
- Propagate the beam with the introduced energy spread through the main dipole;
- Observe the desired longitudinal beam profile.

To measure the slice emittance, utilize the quadrupole located at the point of zero dispersion, and performe a quadrupole scan for various phases of the linac.

Possible reasons to investigate: slice emittance

- For every quadrupole setting, record the corresponding beam profile.
- Slice all of the profiles.
- For each slice plot square of the RMS beam size as a function of the quadrupole strength.
- Fit the data to calculate the emittance.

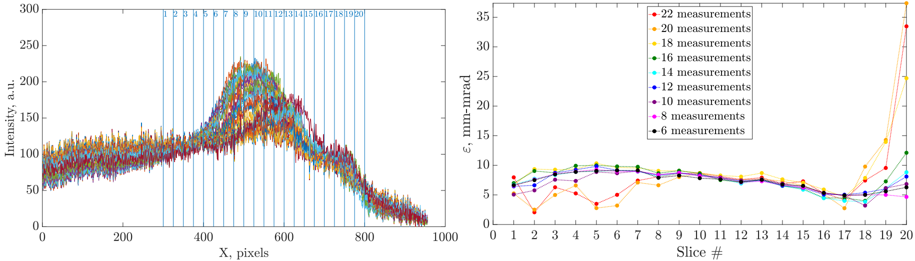

The slice emittance in the central part of the beam doesn't show any variations which could have led to a reduction of the ion imprint.

Possible reasons to investigate

1. ~~Energy difference between the ion and electron beams was larger than 3%.~~
2. ~~Transverse overlap between the bunches was reduced and therefore was insufficient for the interaction.~~
3. FEL was operating in saturation.
4. High initial noise level in the electron beam was present.

Possible reasons to investigate

1. ~~Energy difference between the ion and electron beams was larger than 3%.~~
2. ~~Transverse overlap between the bunches was reduced and therefore was insufficient for the interaction.~~
3. ~~FEL was operating in saturation.~~
4. High initial noise level in the electron beam was present.

Possible reasons to investigate

1. ~~Energy difference between the ion and electron beams was larger than 3%.~~
2. ~~Transverse overlap between the bunches was reduced and therefore was insufficient for the interaction.~~
3. ~~FEL was operating in saturation.~~
4. High initial noise level in the electron beam was present:
    - Modulation in e-beam induced by structures in the drive laser pulse.
    - Longitudinal instability driven by wake fields induced by components of vacuum chambers and RF cavities
    - Instability in dogleg driven by coherent synchrotron radiation in dogleg.

Possible reasons to investigate

1. ~~Energy difference between the ion and electron beams was larger than 3%.~~
2. ~~Transverse overlap between the bunches was reduced and therefore was insufficient for the interaction.~~
3. ~~FEL was operating in saturation.~~
4. High initial noise level in the electron beam was present:
    - ~~Modulation in e-beam induced by structures in the drive laser pulse.~~
    - Longitudinal instability driven by wake fields induced by components of vacuum chambers and RF cavities.
    - Instability in dogleg driven by coherent synchrotron radiation in dogleg.

Wakefields

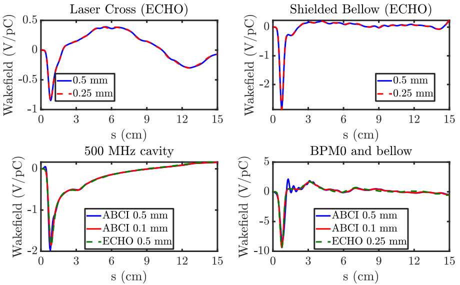

Wake potential in the elements of the laser cross and buncher assembly.

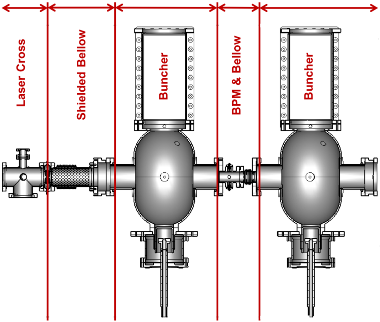

- The simulations showed a good agreement between the two codes.
- Wake fields were calculated for every element of the CeC beam line.
- The highest amplitude of the wake field was observed at the transition between the two bunching cavities.

Wakefields

IMPACT-T simulations performed by Dr. Yichao Jing showed that introduction of the wake fields into the simulation didn't result in a significant change of the beam dynamics in the system.

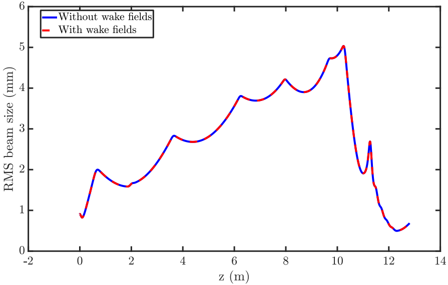

RMS beam size in the LEBT section with and without wake fields.

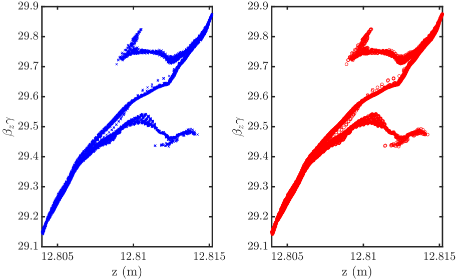

Longitudinal phase space at the exit of the 5-cell cavity.

Possible reasons to investigate

1. ~~Energy difference between the ion and electron beams was larger than 3%.~~
2. ~~Transverse overlap between the bunches was reduced and therefore was insufficient for the interaction.~~
3. ~~FEL was operating in saturation.~~
4. High initial noise level in the electron beam was present:
    - ~~Modulation in e-beam induced by structures in the drive laser pulse.~~
    - ~~Longitudinal instability driven by wake fields induced by components of vacuum chambers and RF cavities.~~
    - Instability in dogleg driven by coherent synchrotron radiation in dogleg.

Possible reasons to investigate

1. ~~Energy difference between the ion and electron beams was larger than 3%.~~
2. ~~Transverse overlap between the bunches was reduced and therefore was insufficient for the interaction.~~
3. ~~FEL was operating in saturation.~~
4. High initial noise level in the electron beam was present:
    - ~~Modulation in e-beam induced by structures in the drive laser pulse.~~
    - ~~Longitudinal instability driven by wake fields induced by components of vacuum chambers and RF cavities.~~
    - ~~Instability in dogleg driven by coherent synchrotron radiation in dogleg.~~

?

First observations of PCI

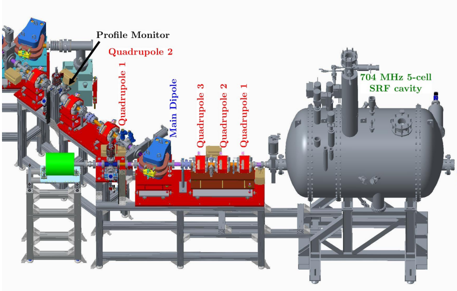

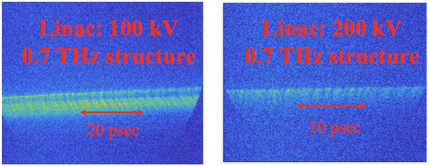

Time profiles showing the dependence of the time resolution on the linac voltage.

Dependence of the dipole radiation on focusing by LEBT 5 solenoid: 7800 bunches, 0.6 nC/bunch:

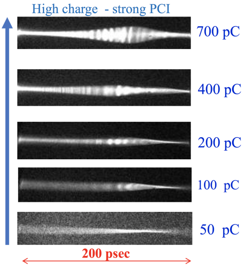

$I_{sol} = 3.625$ A

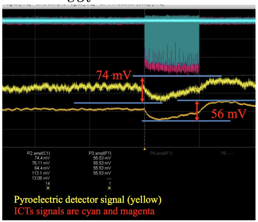

$I_{sol} = 3.675$ A

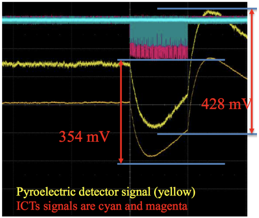

PCI in an uncompressed beam

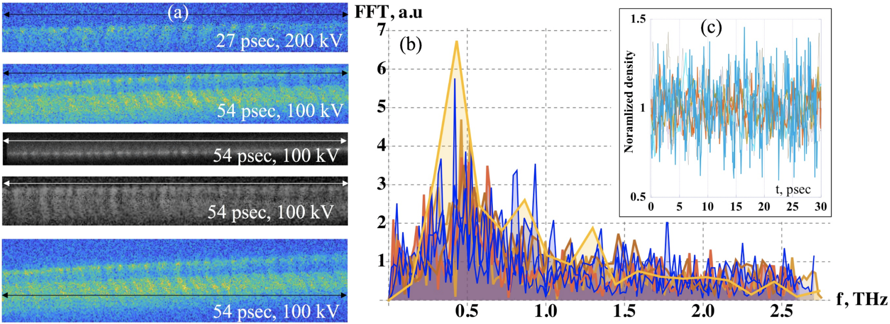

- Time profiles of 1.75 MeV electron bunches with charge per bunch from 0.45 nC to 0.7 nC were measured.
- Compared the spectra of measured bunch density modulation and PCI spectrum simulated by Dr. Jun Ma with SPACE.

Plasma-Cascade Instability (PCI)

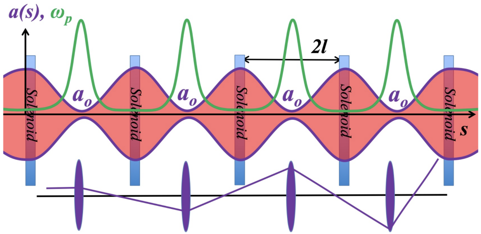

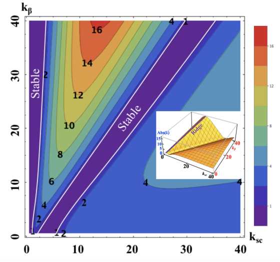

Propagating beam experiences density modulation with period of $T = \dfrac{2l}{\gamma v}$:

$$n_0(s) = \frac{I}{ev}\frac{1}{\pi a^2(s)}$$

Cold beam model:

$$n(s,t) = n_0(s)\left(1 + \tilde{\eta}(s,t)\right)$$

$$\boxed{\frac{\partial n}{\partial t} + \nabla \cdot (n\vec{v}) = 0}$$

$$\frac{d^2\tilde{\eta}}{ds^2} + k_p^2(s)\tilde{\eta} = 0, \text{ with } k_p^2(s) = \frac{4\pi e^2 n_0(s)}{\gamma\gamma_z^2(s) m v^2}$$

$$\boxed{\frac{d^2\hat{a}}{d\hat{s}^2} - \frac{k_{sc}^2}{\hat{a}} - \frac{k_\beta^2}{\hat{a}^3} = 0, \quad \frac{d^2\tilde{q}_k}{d\hat{s}^2} + \frac{2k_{sc}^2}{\hat{a}^2}\tilde{q}_k = 0.}$$

$$\hat{a} = \frac{a}{a_0}, \quad \hat{s} = \frac{s}{l}$$

$$k_{sc} = \sqrt{\frac{2}{\beta^3\gamma^3}\frac{I_0}{I_a}\frac{l^2}{a_0^2}}, \quad k_\beta = \frac{\varepsilon l}{a_0^2}$$

PCI supression

Dr. Yichao Jing has shown through the IMPACT-T simulations that the PCI can be suppressed by the choice of lattice.

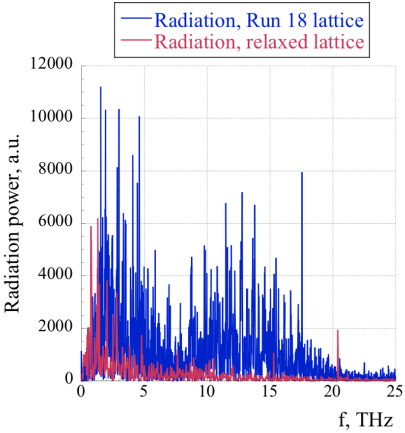

During the Run 2019 we were able to demonstrate the ability of having a quite beam.

PCI applications → ACeC

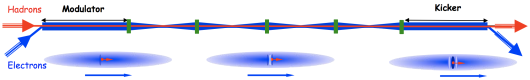

Changing CeC amplifier: FEL → PCA

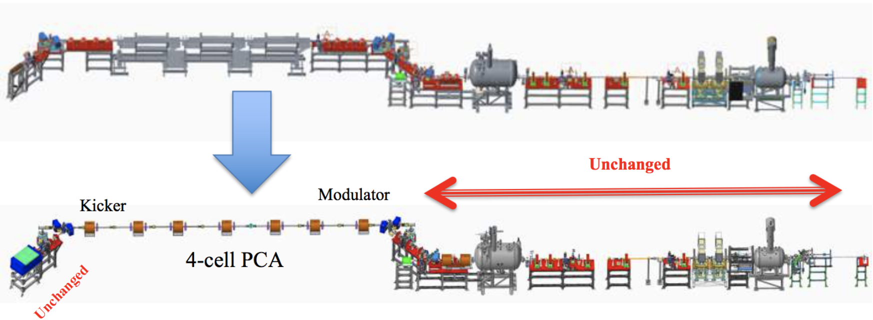

- Mechanical design of the new CeC system is completed.
- New laser system is procured and commissioned.
- All new vacuum chambers with beam diagnostics are built and installed.
- All solenoids are designed, manufactured, delivered and underwent magnetic measurements.
- Assembly of the ACeC can be completed during this year.

Conclusions

- Accelerator delivered the beam with parameters suitable for the CeC PoP experiment:
  - Electron normalized emittance as low as 0.35 mm-mrad was measured
- We were unable to demonstrate the imprint of the hadrons on the electron beam due to the discovered Plasma Cascade Instability
- PCI was experimentally confirmed in the dedicated studies and methods for it suppression were developed
- The PCI will be utilized for the advanced CeC system

References

- Vladimir N. Litvinenko and Yaroslav S. Derbenev, *Coherent Electron Cooling*, Physicsl Review Letters, March 2009;
- V.N. Litvinenko et.al., *Coherent Electron Cooling Demonstration Experiment*, IPAC'11, San Sebastian, Spain, 2011;
- S. Belomestnykh et.al., *SRF and RF systems for CeC PoP experiment*, NAPAC'13 Pasadena, CA, 2013;
- I. Pinayev et.al., *First results of the SRF gun test for CeC PoP*, IPAC'16, Busan, Korea, 2016;
- I. Pinayev et.al., *Commissioning of the CeC PoP accelerator*, NAPAC'16, Chicago, IL, 2016;
- S. Belomestnykh et.al., *Commissioning of the 112 MHz SRF gun*, SRF2015, Canada, 2015;
- I. Pinayev et.al., *Performance of CeC PoP Gun During Commissioning*, NAPAC'16, Chicago, IL, 2016;
- H. Padamsee, *RF Superconductivity*, 2009;
- T.P. Wangler, *RF Linear Accelerators*, 2008.

IR Diagnostics during Run19

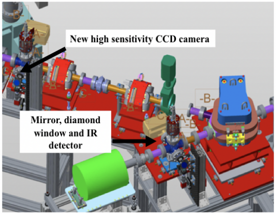

- Utilized high-sensitivity CCD camera for the dogleg profile monitor
- YAG was removed from low-power dump profile monitor. Viewport was replaced with CVD diamond window. IR detector was installed. Mesh was installed to suppress THz radiation.

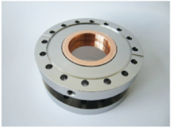

1” CVD diamond window covered with 1.4 mm x 1.4 mm metal mesh to suppress GHz radiation

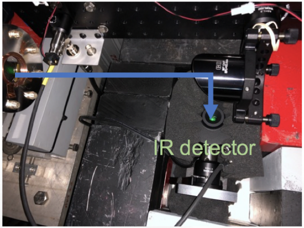

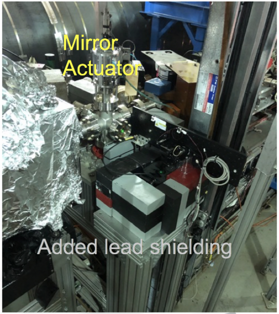

Baseline (shot noise level) measurements

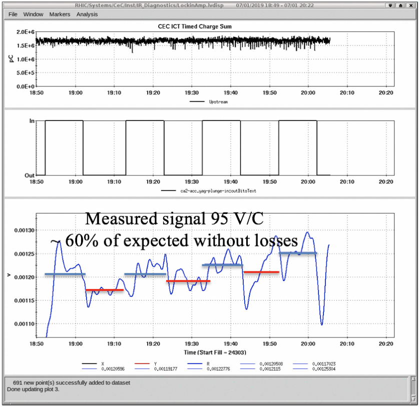

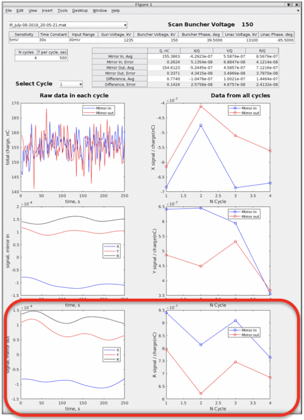

The base line was measured for modestly (4-fold) compressed beam with 1.5 and 0.3 nC charges per bunch in relaxed LEBT lattice. Averaged over 4 long scans the lock-in amplifier MDM signal was **105 V/C (24 μW/A) with RMS error of 15 V/C (3 μW/A)** This value is at 40% level of synchrotron radiation that reaches the Cu mirror

LEBT Optimization

Regular Run18 Lattice

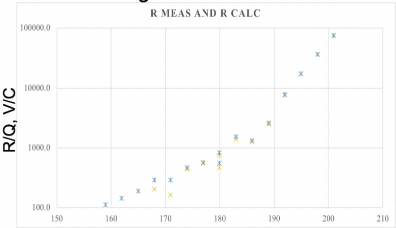

Buncher voltage setting, kV

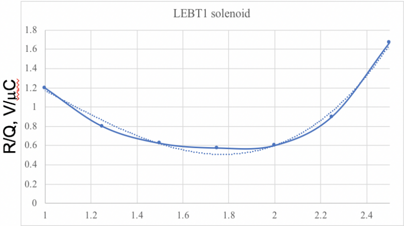

Solenoid current, A

As a result of optimization we were able to achieve the FIR signal only factor two above shot noise level.

The optimized set-up has rather flat response of the noise on the variation of the solenoid current leaving sufficient headroom for optimizing other beam parameters.

Personal Contribution

1. Thorough investigation of multipacting in the 113 MHz photoinjector through the simulations and experiment.
2. Comprehensive study of beam dynamics in the photoinjector.
3. Beam dynamics simulations in the CeC accelerator.
4. Analysis of wake fields in the CeC beamline.
5. Participation in the CeC PoP commissioning.

Linac phase scan

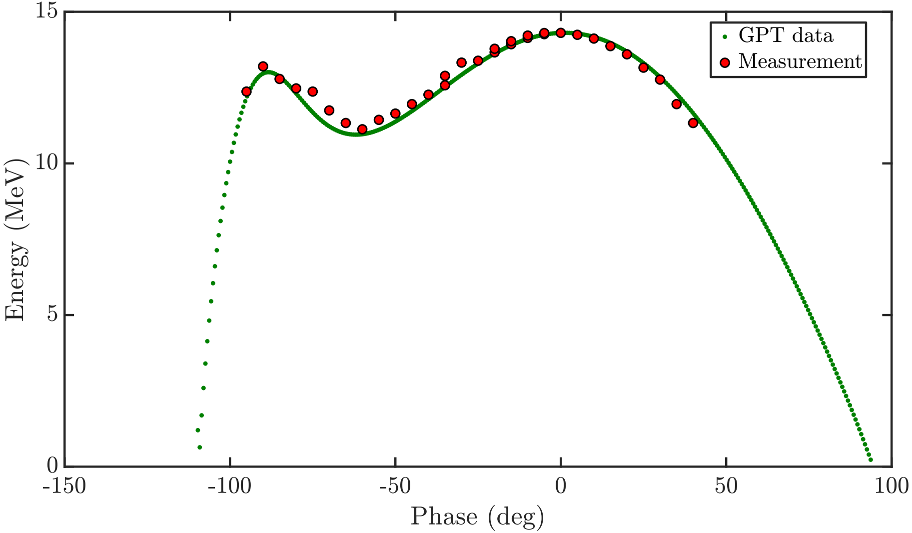

Back-Up: Beam Parameters for Self-Consistent Simulation

Parameters of the beam.

Parameter	Value
Total Charge, nC	0.5
Initial Velocity, β_z	0.003
Type of radial Distribution	Uniform
Radius, mm	1.5
Type of Longitudinal Distribution	Flat Top
Duration of the flat top, ns	0.5
Rise/Drop time, ns	0.005

Back-Up: Summary of the SRF guns

		Elliptical Cavity + NC cathodes			DC-SC	Quarter Wave SRF guns			Elliptical Cavity + SC cathodes	
Parameter	**Units**	**FZD**	**BNL/AES**	**HZB BerlinPro**	**PKU gun**	**NPS 500MHz**	**WiFEL 200MHz**	**BNL 112MHz**	**Pb/Nb hybrid gun**	**HZB HoBiCat**
Beam kinetic energy, V_c	MeV	9.4	2	≤ 3.5	5	1.2	4.0	2.7 (2)	~5	≤ 3.5
Max bunch charge, Q_{max}	nC	1 / 0.077	5 / 0.7	0.077	0.1	1	0.2	5 (2)	1	0.015
Norm. trans. emittance, $□_{n,t}$	mm mrad	2.5 / 1	5 / 1.4	1	1.2	4	0.9	3 (2)	1	1
Average beam current, I_b	mA	1 / 0.5	50 / 500	100	1-5	1	1.0	-	<1 rather 0.1	0.0045
Peak current, I_{pk}	A	67 / 20	166 / 70 (10)	4	20	50	50	-	50	6
Photocathode		Cs_2Te	CsK_2Sb	CsK_2Sb	Cs_2Te	tbd	Cs_2Te	tbd	Pb	Pb
Quantum efficiency, Q.E.	%	1	18	10	1-5	tbd	1	tbd	0.0017	$5x10^{-2}$
Driving laser wavelength, □	nm	263	355	527	266	tbd	266	tbd	213	260
Pulse duration (FWHM)	ps	15 / 4	30 / 20 (10)	≤ 20	5	10 – 40	0.1	270 (2)	<20	2 to 3
Bunch repetition rate, f_{rep}	MHz	0.5 / 13	10 / 704	≤ 1300	81.25	10^{-5} – 100	5	9.4 (2)	<1 rather 0.1	0.030
Gun frequency, f_0	MHz	1300	703.75	1300	1300	500	200	112	1300	1300
Operating temperature	K	2	2	2	2	4.2	4.2	4.2	2	2
Dissipated power, P_{diss} at the intrinsic Q_0 of	W	26 @ $1x10^{10}$	4.2 @ $1x10^{10}$	12.1 (1) @ $1x10^{10}$	-	8.6 @ $9.5x10^8$	42 @ $3.2x10^9$	16.6 @ $3.5x10^9$	143 @ $5x10^9$	12.1 (1) @ $1x10^{10}$
Active cavity length, l_{activ}	cm	50	9.5	17.1	41.7	8	19	20 (2)	18.4	17.1
R_{Shunt}/Q_0, r (R_{shunt} from acc. def.)	Ω	334	96 95.2#	189 (4), □=1 101.4#	418, □=1	185, □=1 176.3#	147.8, □=1 118.8#	126.8 126.6#	170, □=1 35.2#	189^4, □=1 101.4#
Transit time factor, V_c/V_0	TTF	0.715	0.888 (3)	0.54 (1)	0.74 (6)	0.94	0.98 (□=1)	0.99	-	0.54 (1)
Stored energy at E_{pk}, U	J	32.4	8.4 / 9.5*	14.8 (1)	-	2.6	107.2	81.4*	87	14.8 (1)
Electric cathode field E_{cath}	MV/m	30	20	≥ 10	~5 (6)	25	45	19.7	50 - 60	≥ 10
Peak electric field, E_{pk}	MV/m	50	35.7	≤ 50	31.8	44	59	51.3	50 - 60	≤ 50
Peak magnetic flux, B_{pk}	mT	110	74	116	74.5	69.1	90.7	97.8	104 - 125	116
Peak magnetic field, H_{pk}	A/m	87535	59000	≤ 92600	59285	55000	72165	78000 (2)	$(83 - 99)x10^3$	≤ 92600
Persons that provided the data via private communication		A. Arnold (1)	I. Ben-Zvi (2) M. Cole (3)	T. Kamps (4) A. Arnold (1)	J. Hao (5) F. Wang (6)	J.W. Lewellen (7) T.L. Grimm (8)	B. Legg (9)	A. Burril (10) I. Ben-Zvi (2)	J. Sekutowicz (11)	T. Kamps (4) A. Arnold (1)

Cooling Methods

Existing cooling methods are not sufficient:

- Electrons and positrons have natural strong cooling mechanism: Synchrotron Radiation ($\sim$ milliseconds)
- Synchrotron Radiation will not help to cool hadrons at the currently available energies
- Main limitation of electron cooling is its rapidly falling efficiency with the increase of the beam energy $\tau \sim \gamma^{7/2}$
- Stochastic cooling (for a fixed bandwidth) is limited by the fact that its cooling time directly proportional to linear density of the particles and modern proton beams are simply too dense.

Cooling rate in hours for various cooling methods.

Machine	Energy, GeV/u	Stochastic Cooling	Synchrotron radiation	Electron cooling	Coherent electron Cooling
RHIC - CeC PoP (Au)	26	-	-	~ 1	10 sec - local, 30 min - bunch
eRHIC (p)	325	~ 100	∞	~ 30	~ 0.1
LHC (p)	7000	~ 1000	13(energy)/26(transverse)	∞	~ 1

Coherent electron Cooling (CeC) and eRHIC

High energy luminosity Electron-Ion Collider requires strong hadron cooling: < 1 min cooling time of 250 GeV protons

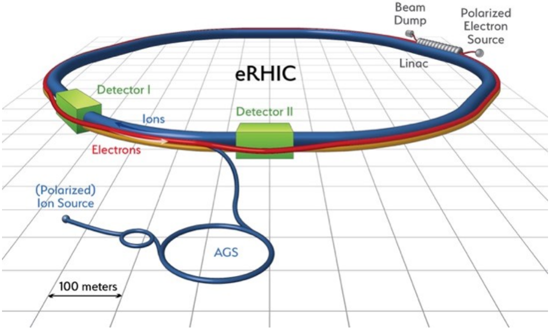

If CeC is successful and fully operational, eRHIC Linac/Ring configuration could reach $2 \cdot 10^{33}$ luminosity with 5 mA polarized electron current.

Coherent electron Cooling (CeC): Modulator

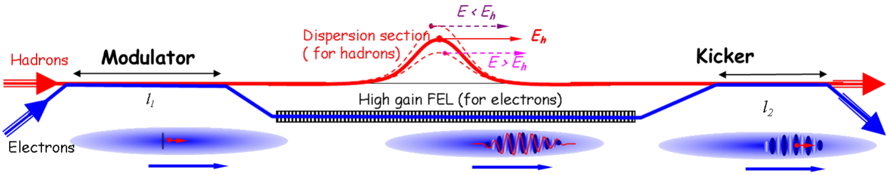

- Each individual hadron attracts surrounding electrons and generates density modulation
- In about a quarter of the plasme period, each hadron is surrounded by a cloud of electrons

$$\omega_p = \sqrt{\frac{4\pi n_e e^2}{\gamma m_e}} \tag{4}$$

- In the co-moving frame, the longitudinal velocity spread is much smaller than that in the transverse direction
- Electron cloud is shaped as a very flat pancake-like shape.

Coherent electron Cooling (CeC): Amplifier

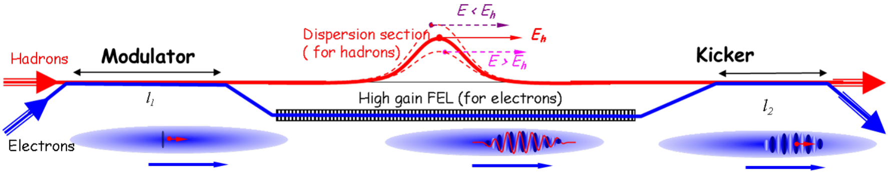

- An FEL is a resonant instability at the wavelength of:

$$\lambda_o = \lambda_w \frac{1 + \langle \vec{a}_w^2 \rangle}{2\gamma^2}, \quad \vec{a}_w = \frac{e\vec{A}_w}{mc^2} \tag{5}$$

- If the longitudinal extent of an induced perturbation is considerably shorter than FEL wavelength, it will be amplified.
- A periodic density modulation generates a periodic longitudinal field.

Fundamental Power Coupler (FPC)/ Frequency Tuner

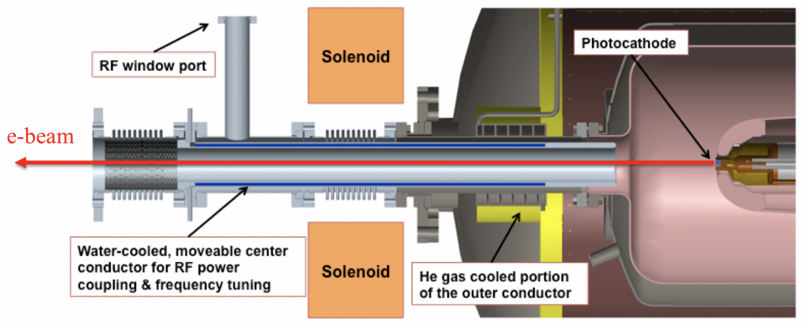

- Fundamental RF power coupling and fine frequency tuning is accomplished via a coaxial beam pipe and the beam exit port.
- With the travel of ± 2 cm, the tuning range is ~ 6 kHz. Rough tuning is accomplished manually via mechanical linkages outside the cryomodule.
- The center conductor and RF windows are water-cooled. The outer conductor copper coated bellows are air-cooled.
- The center conductor is gold-plated to reduce heat radiated into the SRF cavity.

Cathode Stalk Design

- The cathode stalk is a hollow center conductor of the coaxial line formed by the stalk and the cavity.
- The stalk is shorted at one end and is approximately half wavelength long.
- A quarter-wave step from the short creates an impedance transformer $\rightarrow$ reduces RF losses in the stalk from $\sim$65 W to $\sim$25 W.
- The gold plating reduces radiation heat load from the stalk.

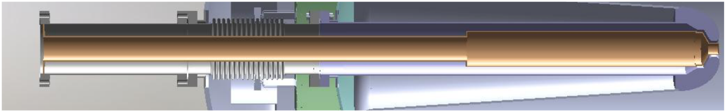

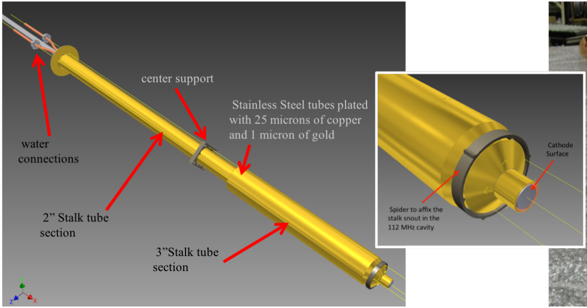

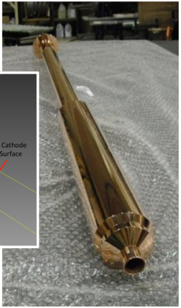

Cathode Recess

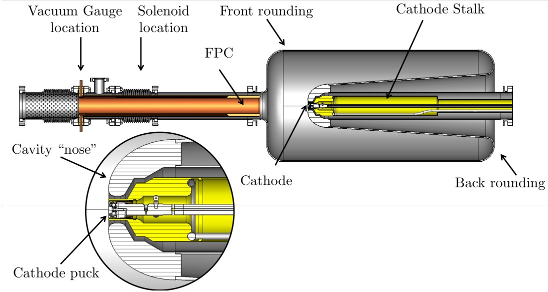

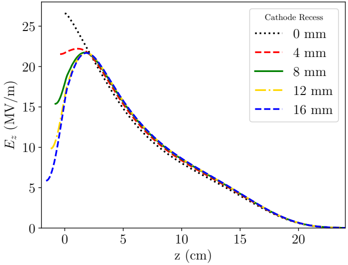

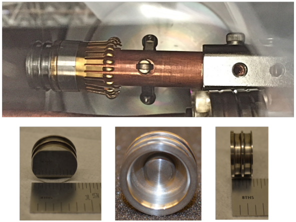

Cathode puck

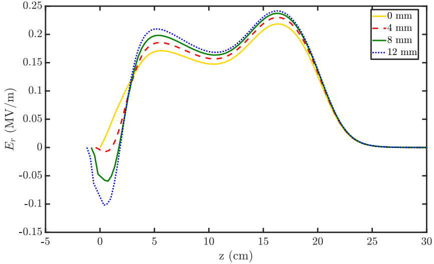

Cathode Recess

Magnification

ratio of the beam position at the YAG screen and the laser spot position.

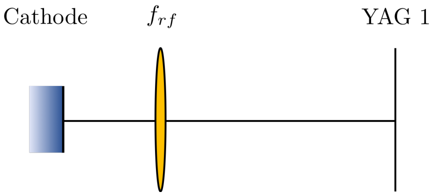

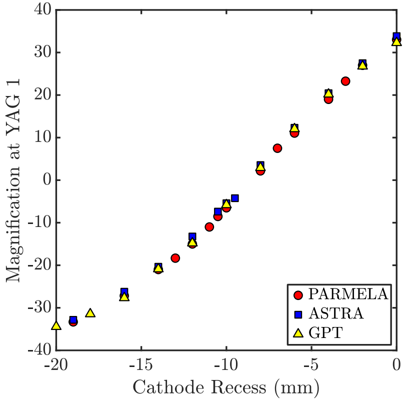

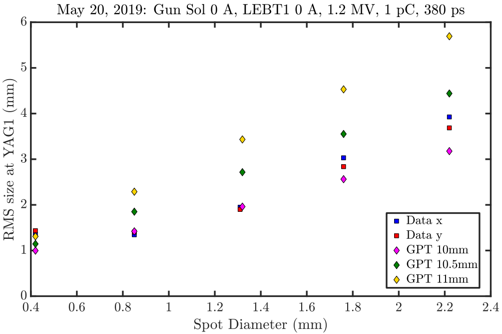

Electrical Axis of the Gun

In order to determine the electrical axis of the gun:

- change the beam rigidity $\frac{p}{e} = B\rho$ by scanning the voltage of the gun
- measure the position of the beam center at the first profile monitor

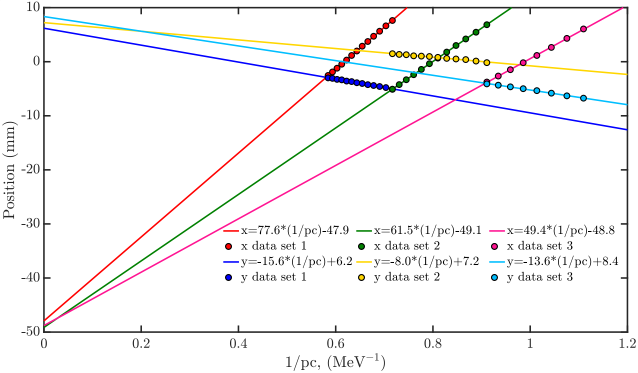

The y-intercept gives the direction of the gun axis for an infinitely rigid beam: horizontal angle of -11.1±0.1 mrad, and vertical angle of +1.6±0.2 mrad.

Multipacting Simulations

CST Particle Studio

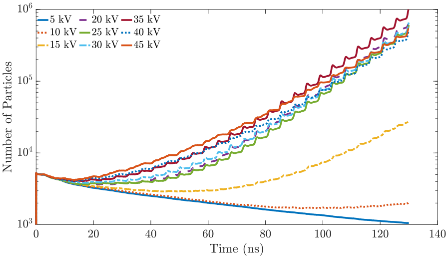

$$N_e(t) = N_0 e^{\alpha t}$$

ACE3P (Track3P)

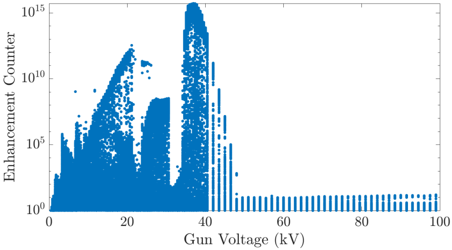

$$EC = \delta_1 \times \delta_2 \times \ldots \times \delta_n$$

Multipacting Simulations

CST Particle Studio

ACE3P (Track3P)

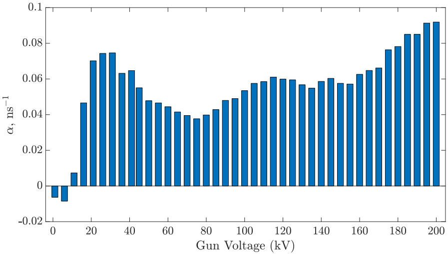

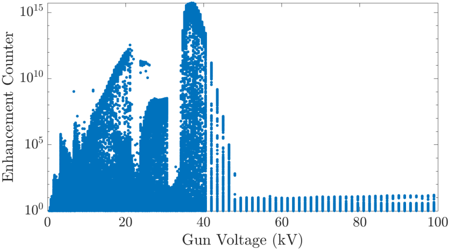

$$N_e(t) = N_0 e^{\alpha t}$$

$$EC = \delta_1 \times \delta_2 \times \ldots \times \delta_n$$

Simulation results: not so consistent.

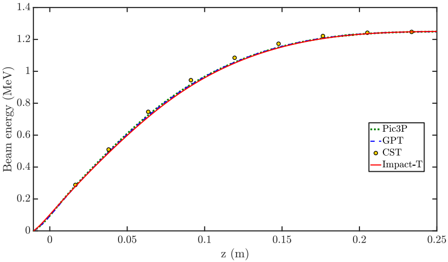

Beam energy vs. z in the gun.

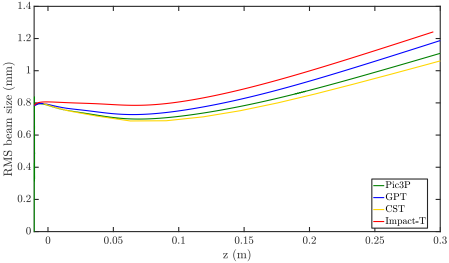

RMS beam size evolution in the gun.

Parameter	**CST PS**	**Pic3P**	**GPT**	**IMPACT-T**
Specifics of the algorithm				
Equations solved	Maxwell	Maxwell	Poisson	Poisson
Wakefileds	✓	✓	×	×
Space charge	✓	✓	✓	✓
Retardation effects	✓	✓	×	×
Image charge	Real geometry	Real geometry	Flat wall	Flat wall

XY distribution at the gun exit

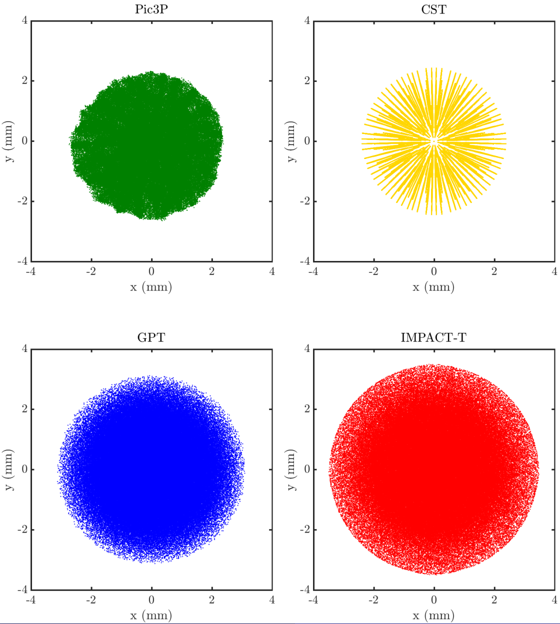

XY distribution at the gun exit

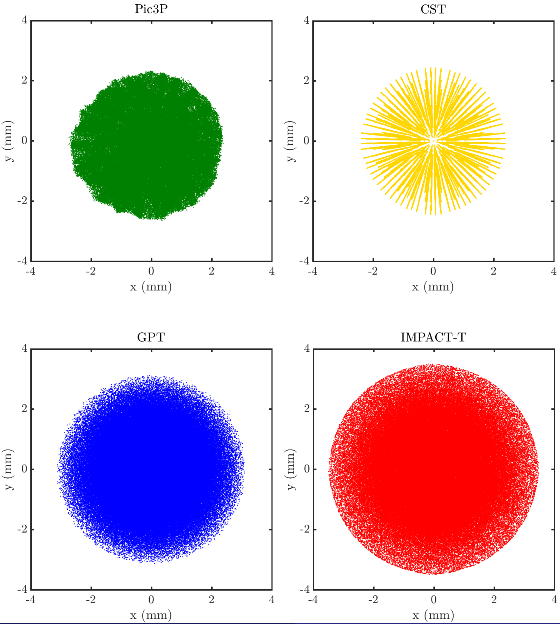

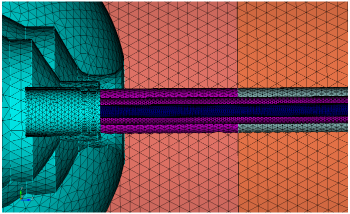

Tetrahedral meshing in Pic3P.

XY distribution at the gun exit

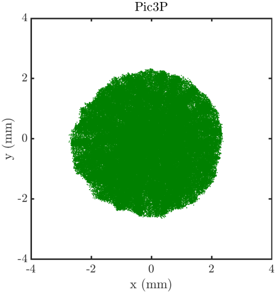

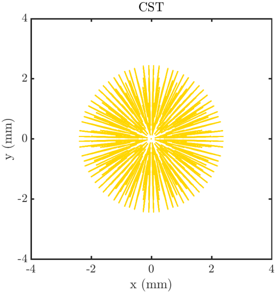

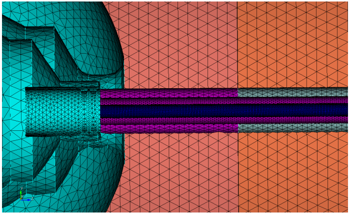

Tetrahedral meshing in Pic3P.

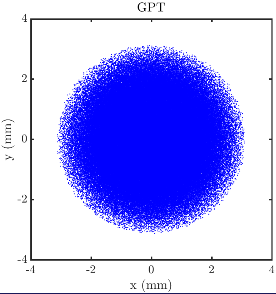

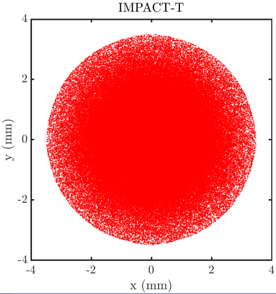

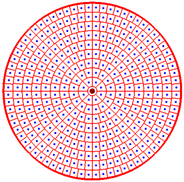

Particle source in CST.

XZ distribution at the gun exit

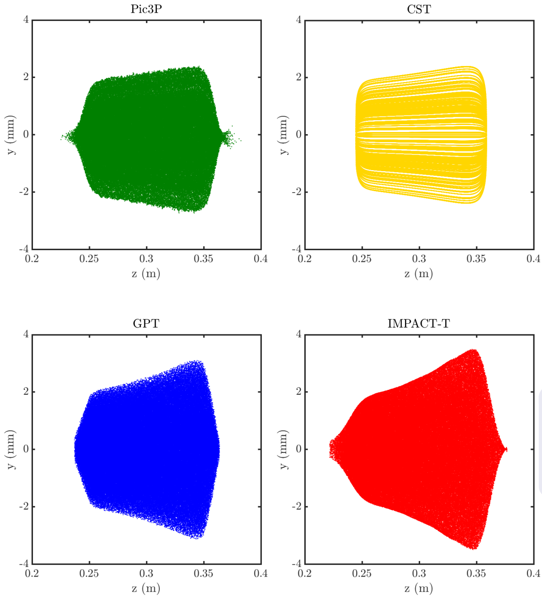

Longitudinal distribution

- **Pic3P, GPT, IMPACT-T:** uniform with rise/drop time
- **CST:** truncated Gaussian.

CST and **Pic3P** are excluded from the race for the best initial particle distribution.

Emittance compensation

Goal: optimize the normalized RMS emittance at YAG 1 by appropriate choice of the gun and LEBT 1 soloenoids.

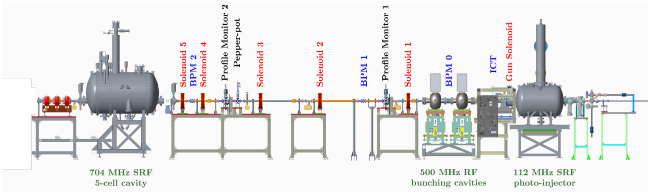

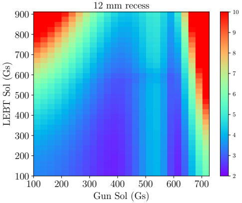

Parameter	Value
Radius of the laser spot, mm	0.25-2.5
Pulse length, ps	400
Bunch charge, pc	10-600
Gun Voltage, MV	1.25
Cathode recess, mm	0-12

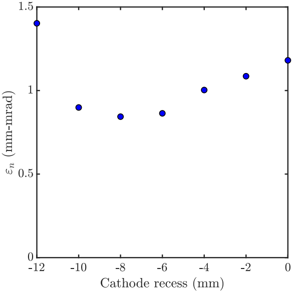

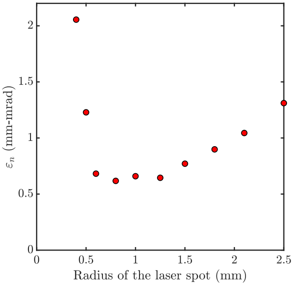

Emittance compensation

Goal: optimize the normalized RMS emittance at YAG 1 by appropriate choice of the gun and LEBT 1 soloenoids.

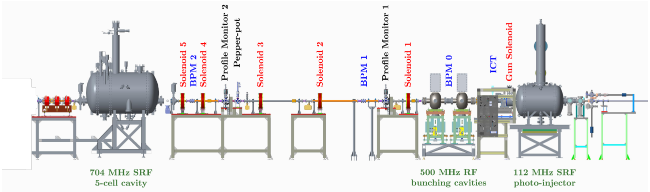

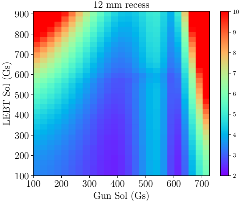

Parameter	Value
Radius of the laser spot, mm	0.25-2.5
Pulse length, ps	400
Bunch charge, pc	10-600
Gun Voltage, MV	1.25
Cathode recess, mm	0-12

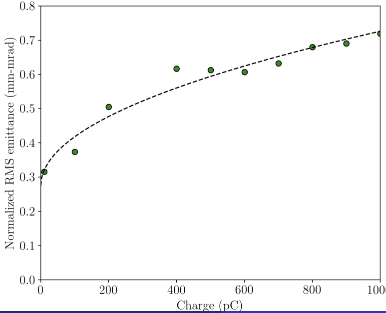

113 MHz Photoinjector: excellent performance!

- Gun energy: 1.25 MeV.
- Laser spot on cathode RMS size: 0.8mm (3.2 mm diameter)
- Bunch charge: 600 pC.
- Bunch length: 400 ps.
- Gun solenoid: 8.6 A.
- LEBT1 solenoid varied from -7 to -1 A (left) and 1 to 7 A (right).

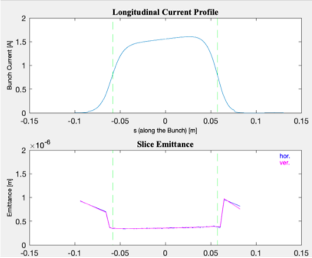

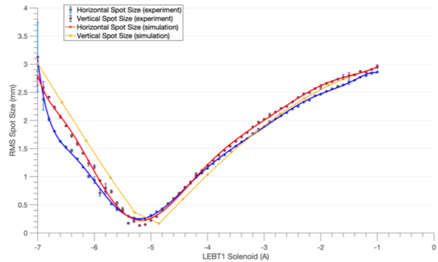

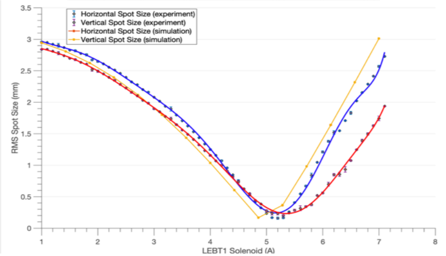

Projected normalized emittance—0.57 mm-mrad.

Normalized core slice emittance—0.35 mm-mrad.

Emittance study: 100 pC

The simulation results of the LEBT scan provide a projected normalized RMS emittance of 0.23 mm-mrad, while the slice emittance demonstrated a uniform core with the slice emittance of about 0.13 mm-mrad.

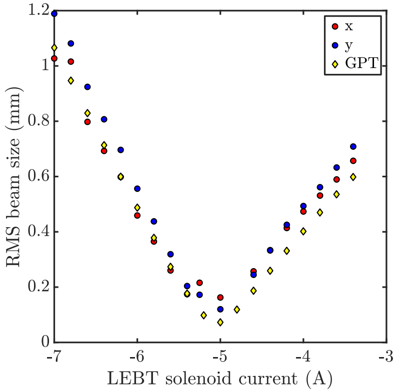

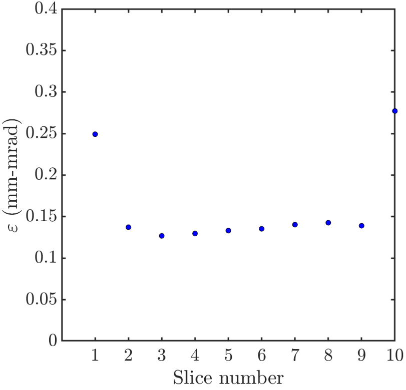

Emittance study: 600 pC

The oscillation in the beam emittance after the gun solenoid is the result of the successful emittance compensation.

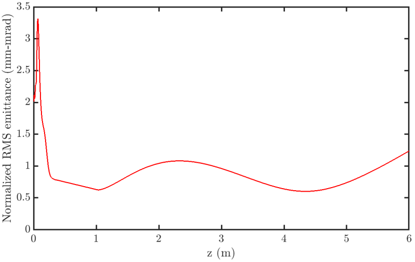

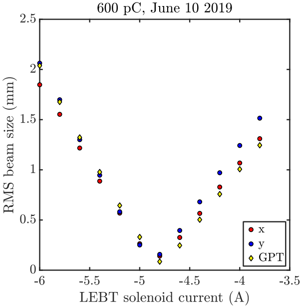

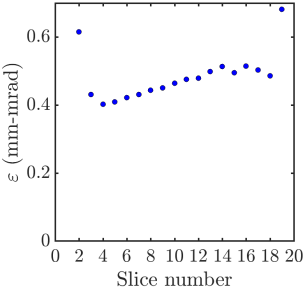

Emittance study: 100 pC with increased spot size

20% increase of the spot size caused an increase in the projected emittance by 32% (0.303 mm-mrad) with the slice emittance of about 0.15 mm-mrad on average.

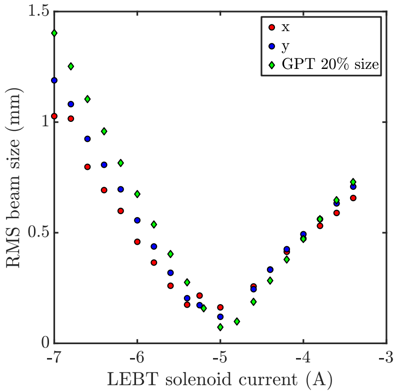

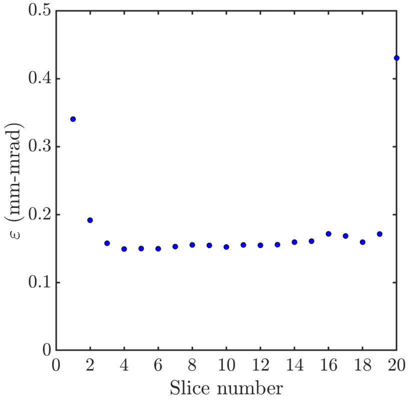

Emittance study: 100 pC

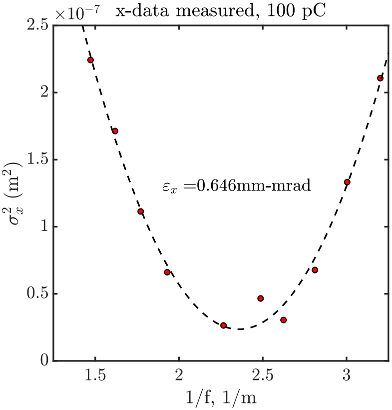

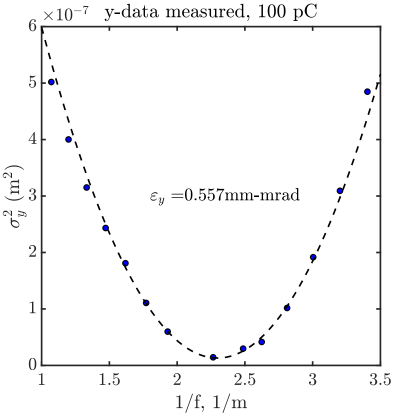

This data set was obtained for a 0.4 ns 100 pC electron beam at 1.25 MV gun voltage, and 1.34 mm diameter of the laser spot at the cathode.

Wakefields

- The beam loses part of its energy to establish EM—wake—fields that remain after the passage of the beam.
- Theses wake fields affect trailing particles of the same beam or the following beam.

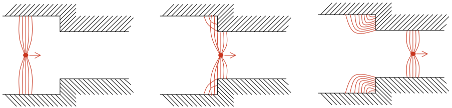

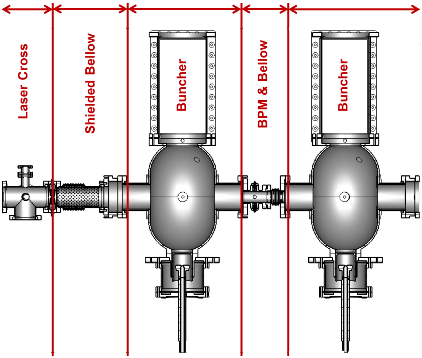

Parameter	ABCI	ECHO 3D
Geometry	Axially symmetric	Full 3D
Beam Duration (ps)	5	5
Simulation Duration (ps)	500	500

Transverse overlap of the electron and ion beams

1. Utilize two quadrupole magnets at the beginning and the end of the common section: the first quadrupole of the modulator section and the last quadrupole of the kicker section.
2. When passing through the center of a quadrupole, the orbit of a charged particle beam doesn't change.
3. Varying the transverse position of a beam, and then observing the effect of the varied field in the quadrupole, find the quadrupole center.
4. Performed for both, the electron and ion beams at the beginning and the end of the common section.

$\checkmark$

Longitudinal overlap of the electron and ion beams

1. Observe the signal from the BPM in the common section.
2. By adjusting the phase shift of the CeC RF system, align the signal from the electron bunch to the center of the ion bunch.

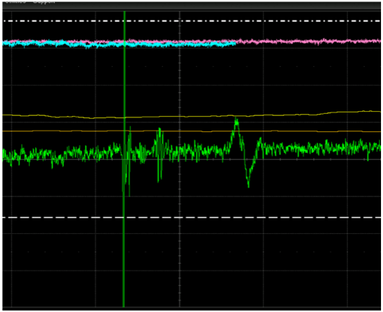

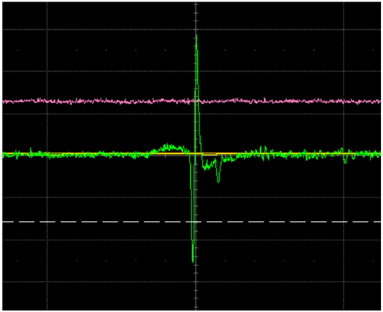

✓

Personal Contribution

1. Thorough investigation of multipacting in the 113 NHz photoinjector through the simulations and experiment.
2. Comprehensive study of beam dynamics in the photoinjector.
3. Beam dynamics simulations in the CeC accelerator.
4. Analysis of wake fields in the CeC beamline.
5. Participation in the CeC PoP commissioning.